Zeitschrift: Eclogae Geologicae Helvetiae

Herausgeber: Schweizerische Geologische Gesellschaft

Band: 86 (1993)

Heft: 3

Artikel: Alluvial fan sedimentation and structure of the southern Molasse Basin

margin, Lake Thun area, Switzerland

Autor: Schlunegger, Fritz / Matter, Albert / Mange, Maria A.

DOI: https://doi.org/10.5169/seals-167260

Nutzungsbedingungen

Die ETH-Bibliothek ist die Anbieterin der digitalisierten Zeitschriften auf E-Periodica. Sie besitzt keine Urheberrechte an den Zeitschriften und ist nicht verantwortlich für deren Inhalte. Die Rechte liegen in der Regel bei den Herausgebern beziehungsweise den externen Rechteinhabern. Das Veröffentlichen von Bildern in Print- und Online-Publikationen sowie auf Social Media-Kanälen oder Webseiten ist nur mit vorheriger Genehmigung der Rechteinhaber erlaubt. Mehr erfahren

Conditions d'utilisation

L'ETH Library est le fournisseur des revues numérisées. Elle ne détient aucun droit d'auteur sur les revues et n'est pas responsable de leur contenu. En règle générale, les droits sont détenus par les éditeurs ou les détenteurs de droits externes. La reproduction d'images dans des publications imprimées ou en ligne ainsi que sur des canaux de médias sociaux ou des sites web n'est autorisée qu'avec l'accord préalable des détenteurs des droits. En savoir plus

Terms of use

The ETH Library is the provider of the digitised journals. It does not own any copyrights to the journals and is not responsible for their content. The rights usually lie with the publishers or the external rights holders. Publishing images in print and online publications, as well as on social media channels or websites, is only permitted with the prior consent of the rights holders. Find out more

Download PDF: 29.11.2025

ETH-Bibliothek Zürich, E-Periodica, https://www.e-periodica.ch

Alluvial fan sedimentation and structure of the southern Molasse Basin margin, Lake Thun area, Switzerland

by Fritz Schlunegger¹, Albert Matter¹ and Maria A. Mange²

Key words: Molasse, alluvial fans, foreland basin, sedimentation, tectonics

ABSTRACT

The Chattian Lower Freshwater Molasse (USM) of the Thun area comprises a thick series of continental sediments which occur in three imbricate thrust sheets (Steffisburg, Zulg-Hombach, Blueme) of the Subalpine Molasse and over wide areas of the autochthonous Plateau Molasse. Facies analysis of outcrops, complemented by conglomerate clast counts, sandstone petrography, heavy mineral analysis and data from two deep exploration wells and seismics permit structural restoration of the thrust sheets, correlation of subalpine and autochthonous USM and consequently the reconstruction of the geometry and facies evolution of the alluvial fan systems.

The most complete succession measuring more than 4500 m is preserved in the structurally highest Blueme thrust sheet. It is divided into six informal units which are distinguishable in terms of litho- and petrofacies and which when mapped enable three major (Schwändibach, Honegg, Blueme) and two local (Honegg Marl, Gitzischöpf) fan systems to be recognised.

The small Schwändibach fan consists of the more than 400 m thick Early Chattian Schwändibach Conglomerate, a proximal conglomerate with subordinate sandstone to mudstone interbeds. It interfingers laterally with the larger Honegg fan comprising Homberg Beds and Losenegg Beds which record progradation of the fan. The Homberg Beds measuring 500 m form a relatively fine grained unit made up of channel sandstones with epsilon cross bedding and associated crevasse splay, levee and floodbasin deposits. Single and amalgamated beds of conglomerate account for 60% of the overlying 450 m thick Losenegg Beds. Progradation is recognisable from the coarsening upward trend associated with a change in fluvial style from meandering to sinuous. A mixture of sedimentary and igneous clasts and an apatite-rich heavy mineral assemblage are typical of these older fans.

Separated by a structural discordance and an erosional unconformity from the older fans, the third major fan, the Blueme fan of Late Chattian age, is distinguished by a very different petrofacies with an epidote dominated heavy mineral suite and predominance of igneous clasts in the conglomerates. It consists of the Thun Conglomerate, itself comprised by the Hünibach Conglomerate and the Gunten Quartzite Conglomerate, with a total thickness of more than 4000 m in the centre of the fan. The general coarsening upward trend continues through this unit in parallel with an increasingly more braided depositional pattern indicative of increasing proximality and higher gradient.

The Blueme fan is overlain by the Honegg Marls (240 m) made up of structureless, occasionally laminated or graded marls with few sandstone beds. It contains an apatite-rich heavy mineral suite, and rare ribbon-conglomerates with a high percentage of flysch sandstone clasts. It is followed by the Gitzischöpf Conglomerate (> 250 m) consisting of narrow conglomerate filled channels with lensoid cross-section in a marly background sediment. The petrofacies varies from igneous- to sedimentary-clast conglomerates and from apatite- to epidote-rich heavy mineral suites. These units represent local fans which encroached onto the Blueme fan as it prograded.

The structural restoration reveals strongly diachronous facies relationships in the Lower Freshwater Molasse at the southern basin margin which are the result of large-scale progradation of the fan systems; the Late Chattian

¹⁾ Universität Bern, Geologisches Institut, Baltzerstrasse 1, CH-3012 Bern, Switzerland.

²⁾ University of Oxford, Department of Earth Sciences, Parks Road, Oxford, OX1 3PR, England.

Gunten Quartzite Conglomerate of the Subalpine Molasse correlates with the Burdigalian to Langhian conglomerates of the Plateau Molasse in the Linden-1 well.

The drastic compositional change from the Honegg fan to the Blueme fan at 25 Ma followed by marked fan advance and change in fluvial style are interpreted as the result of the Insubric orogenic phase of backthrusting which caused rapid uplift, expansion of the drainage area from the Penninic into the Austroalpine nappes and increased rates of erosion.

ZUSAMMENFASSUNG

Die Untere Süsswassermolasse (USM) und Obere Meeresmolasse (OMM) am Alpenrand nördlich des Thunersees bestehen aus einer mächtigen Abfolge kontinentaler Sedimente, die einerseits drei Schuppen der Subalpinen Molasse (Steffisburg-, Zulg-Hombach-, Blueme-Schuppe) aufbauen und andererseits in der mittelländischen Molasse weitverbreitet sind. Die sedimentologische und sedimentpetrographische Untersuchung von zwei Oberflächenprofilen sowie der Tiefbohrungen Linden-1 und Thun-1 und die Auswertung des die beiden Bohrungen verbindenden seismischen Profils ermöglichen die palinspastische Rekonstruktion und die Korrelation von subalpiner und mittelländischer USM. Dies gestattet sodann die Rekonstruktion der Geometrie der alluvialen Schuttfächersysteme und der Faziesentwicklung am südlichen Rand des Molassebeckens.

In der Blueme-Schuppe liegt die vollständigste, über 4500 m mächtige USM-Abfolge vor, welche in sechs informelle lithostratigraphische Einheiten unterteilt wird, die sich aufgrund unterschiedlicher Litho- und Petrofazies klar unterscheiden. Deren Auskartierung lässt drei Hauptschuttfächer-Systeme und zwei lokale Schuttfächer erkennen. Der verhältnismässig kleine Schwändibach-Schuttfächer umfasst die mehr als 400 m mächtige Schwändibach-Nagelfluh des frühen Chattian, bestehend vor allem aus proximalen Konglomeraten und untergeordnet Sandstein- und Mergelzwischenlagen. Sie verzahnt sich lateral gegen NE mit den gleichaltrigen Homberg Schichten. Letztere bauen zusammen mit den hangenden Losenegg-Schichten den Honegg-Schuttfächer auf. Die Homberg-Schichten stellen eine 500 m mächtige relativ feinkörnige Abfolge, bestehend aus Rinnensandsteinen mit Epsilon-Schrägschichtung, Durchbruchsfächern sowie Uferwall- und Üeberschwemmungsebenen Ablagerungen dar. Die hangenden 450 m mächtigen Losenegg-Schichten setzen sich dagegen zu über 60 % aus Konglomeraten zusammen. Die gegen oben zunehmend grobkörniger werdenden Sedimente, verbunden mit einer Veränderung des Flussstils von mäandrierend zu schwach gewunden, lassen auf ein Vorrücken des Schuttfächers schliessen. Die beiden Schuttfächer des frühen Chattian sind durch eine Mischung sedimentärer und kristalliner Gerölle und eine Apatitvormacht im Schwermineralspektrum gekennzeichnet.

Eine strukturelle Diskordanz und eine Schichtlücke trennen den dritten der grossen Schuttfächer, Blueme-Schuttfächer genannt, von den älteren Schuttfächern. Dieser im Zentrum über 4000 m mächtige Schuttfächer wird vollständig von der spätchattischen Thuner Nagelfluh, bestehend aus Hünibach und Guntener Quartzit-Nagelfluh. aufgebaut, die mit einer Epidot-reichen Schwermineralassoziation und einer Vormacht der Kristallingerölle eine deutlich andere Petrofazies aufweist. Der allgemeine "coarsening upward" Trend setzt sich in dieser Einheit fort, wobei der Flussstil einen zunehmend verwilderten Charakter annimmt, beides Anzeichen für Progradation des Schuttfächers

Die hangenden Honegg-Mergel (240 m) bestehen aus strukturlosen, gelegentlich laminierten oder gradierten Mergeln mit vereinzelten Sandsteinbänken und seltenen schmalen Konglomeratrinnen. Ihre Petrofazies ist gekennzeichnet durch die Vorherrschaft von Flyschgeröllen und Apatit. Schmale Konglomeratrinnen mit linsenförmigem Querschnitt in einem mergeligen Hintergrundsediment bauen die Gitzischöpf-Nagelfluh auf, die den Abschluss der USM bildet. Ihre Petrofazies variiert von kristallinreichen zu sedimentreichen Konglomeraten und von Epidotzu Apatitvormacht im Schwermineralspektrum. Honegg-Mergel und Gitzischöpf-Nagelfluh stellen Ablagerungen lokaler Schuttfächer dar, die sich seitlich mit dem gleichaltrigen Blueme-Schuttfächer verzahnen und diesen allmählich eindecken.

Die palinspastische Rekonstruktion deckt die stark heterochronen Faziesverhältnisse in der Unteren Süsswassermolasse des südlichen Beckenrandes auf, ein Ergebnis der raschen Progradation der Schuttfächer. Beispielsweise korreliert die spät-chattische Guntener Quarzit-Nagelfluh der subalpinen Molasse mit dem Burdigalian-Langhian-Konglomerat der mittelländischen Molasse in der Bohrung Linden-1.

Der an der Grenze vom frühen zum späten Chattian um 25 Ma festgestellte markante petrofazielle Wechsel, sowie das anschliessende rasche Vorrücken des Blueme-Schuttfächers und die Veränderung des Flussstils werden auf die rasche Heraushebung des internen Alpenkörpers während der insubrischen Phase zurückgeführt. Die Zone des höchsten Abtrags verlagerte sich von den tieferen penninischen Decken gegen Süden, und in der Folge lieferten

die alpinen Flüsse vermehrt kristallinen Detritus der höheren penninischen und der ostalpinen Decken. Daher liegt in der nordalpinen Molasse im Gegensatz zu derjenigen am Alpensüdfuss keine normale "Unroofing"-Sequenz vor.

1. Introduction

The depositional history of the North Alpine Foreland Basin with its deep-water (flysch) phase followed by shallow-water to continental (molasse) sedimentation is largely controlled by the evolution of the Alpine orogenic wedge (Trümpy 1960, Homewood et al. 1986, Sinclair et al. 1991). Orogenic thrust front propagation also caused dissection and frontal accretion of the proximal Molasse sequence. The latter now forms an imbricate stack of thrust slices of the Subalpine Molasse consisting mainly of Lower Freshwater Molasse and some Lower Marine Molasse. Its tectonic separation from the Plateau Molasse, the scarcity of biostratigraphically relevant fauna and flora and rather scarce subsurface information have all hindered reconstructions of the structural and depositional history of the Molasse Basin. Further limitations come from the fact that the southernmost Plateau Molasse is hidden beneath the Subalpine Molasse thrust wedge and from the uncertainties regarding thrust geometry and amount of crustal shortening (Burkhard 1990).

Four lithostratigraphic groups are generally distinguished in the North Alpine Foreland Basin (Matter et al. 1980): Lower Marine Molasse (UMM), Lower Freshwater Molasse (USM), Upper Marine Molasse (OMM), and Upper Freshwater Molasse (OSM). As pointed out by Sinclair et al. (1991), the North Helvetic Flysch, representing the initial deep-water phase of the basin, should be distinguished as a fifth group. These five groups record two large-scale shallowing- and coarsening-upward cycles separated by the basal Burdigalian unconformity. The upper part of each cycle is represented by continental deposits (Freshwater Molasse). However, in the proximal areas of the basin both, the Lower Freshwater Molasse and the overlying Upper Marine Molasse consist of alluvial fan clastics (Berli 1985, Bolliger et al. 1988, Hurni 1992) and as yet no stratigraphic gap related to the Burdigalian unconformity has been recognised.

As early as 1825 Studer had noticed the general coarse-grained character of the Molasse in the Thun area and the fact that conglomerates increase in abundance up-section. Renz (1937) interpreted this 3-4 km thick conglomeratic sequence as an alluvial fan (Blume fan). Although the structure and lithostratigraphy of the Molasse north of Lake Thun are fairly well known due to regional studies by Beck (1923, 1946), Haus (1937), Beck & Rutsch (1958) and Scherer (1966), a detailed sedimentological investigation of the Subalpine Lower Freshwater Molasse was carried out only recently (Schlunegger 1991). The deep well Linden-1 (Maurer et al. 1978) sunk in the Plateau Molasse and the new well Thun-1 (Micholet 1992) which explored the Subalpine Molasse and the autochthonous Molasse beneath, and related seismic data (Vollmayr 1992) now provide excellent subsurface control.

This study investigates the continental deposits within a segment of the southern margin of the Molasse Basin near Thun which encompasses the Subalpine and the Plateau Molasse (Fig. 1). It focusses on the Chattian Lower Freshwater Molasse of the Subalpine zone and the Chattian-Langhian Plateau Molasse. The theme is the structural restoration of the Subalpine Molasse and the reconstruction of the geometry and sedi-

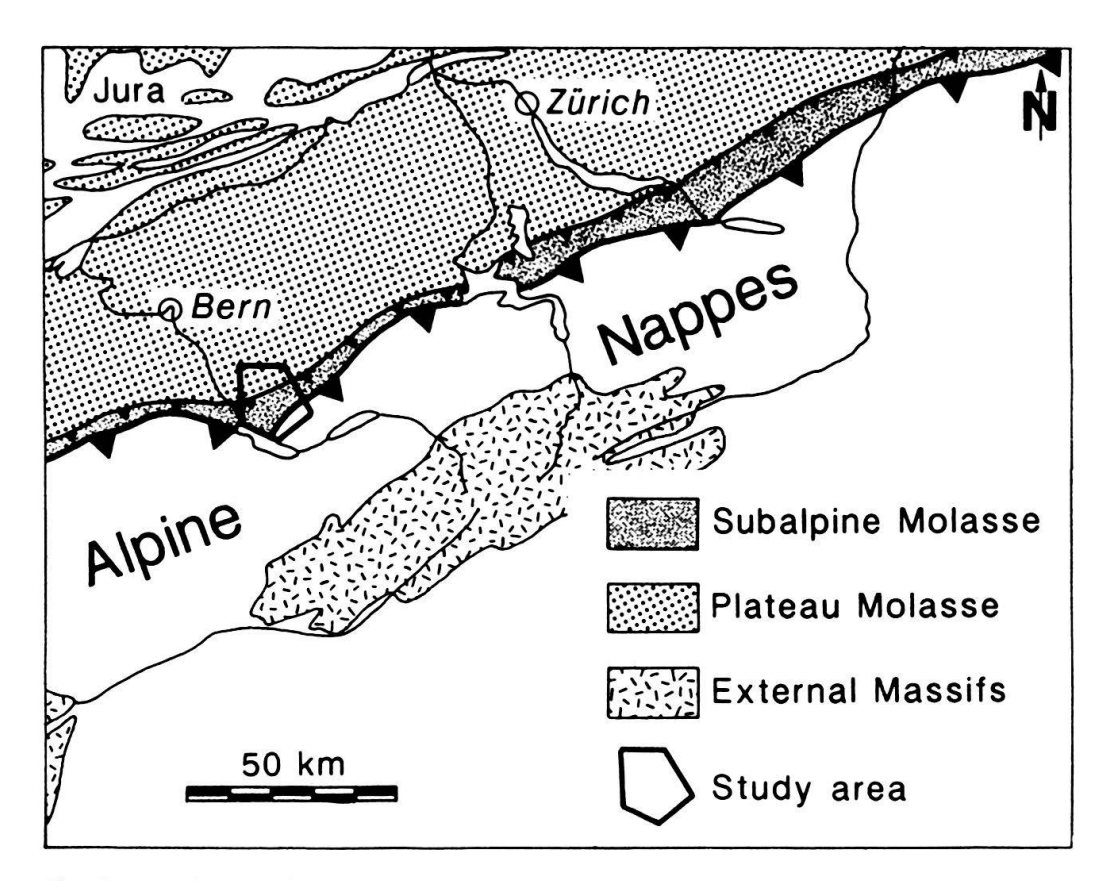


Fig. 1. Simple tectonic map of central northern Switzerland, with study area indicated.

mentological evolution of the alluvial fans at the southern basin margin. Possible controls of Alpine events on alluvial sedimentation will also be explored.

2. Methods

The Molasse of the Thun region was mapped and sedimentological sections were measured along the Prässerebach river cut and northeast of Thun which expose almost the entire Lower Freshwater Molasse of the Subalpine zone. These sections were sampled for heavy mineral analysis, modal analysis of sandstones and for analysis of conglomerate clast composition (Schlunegger 1991). In addition, heavy mineral analyses of cutting samples from the well Thun-1 were carried out. These new data permitted the lithostratigraphic division of the borehole section, its correlation with Linden-1 and with the Prässerebach and Thun sections as well as the structural interpretation of the seismic line linking both wells.

For each location, the *conglomerate petrofacies* was determined in the laboratory on 160 to 200 clasts with a long diameter > 2 cm which were collected from 1 m² of outcrop. The long axis of the five largest clasts was measured to determine maximum average clast size. The clast count data are given on Table 1 (after the references).

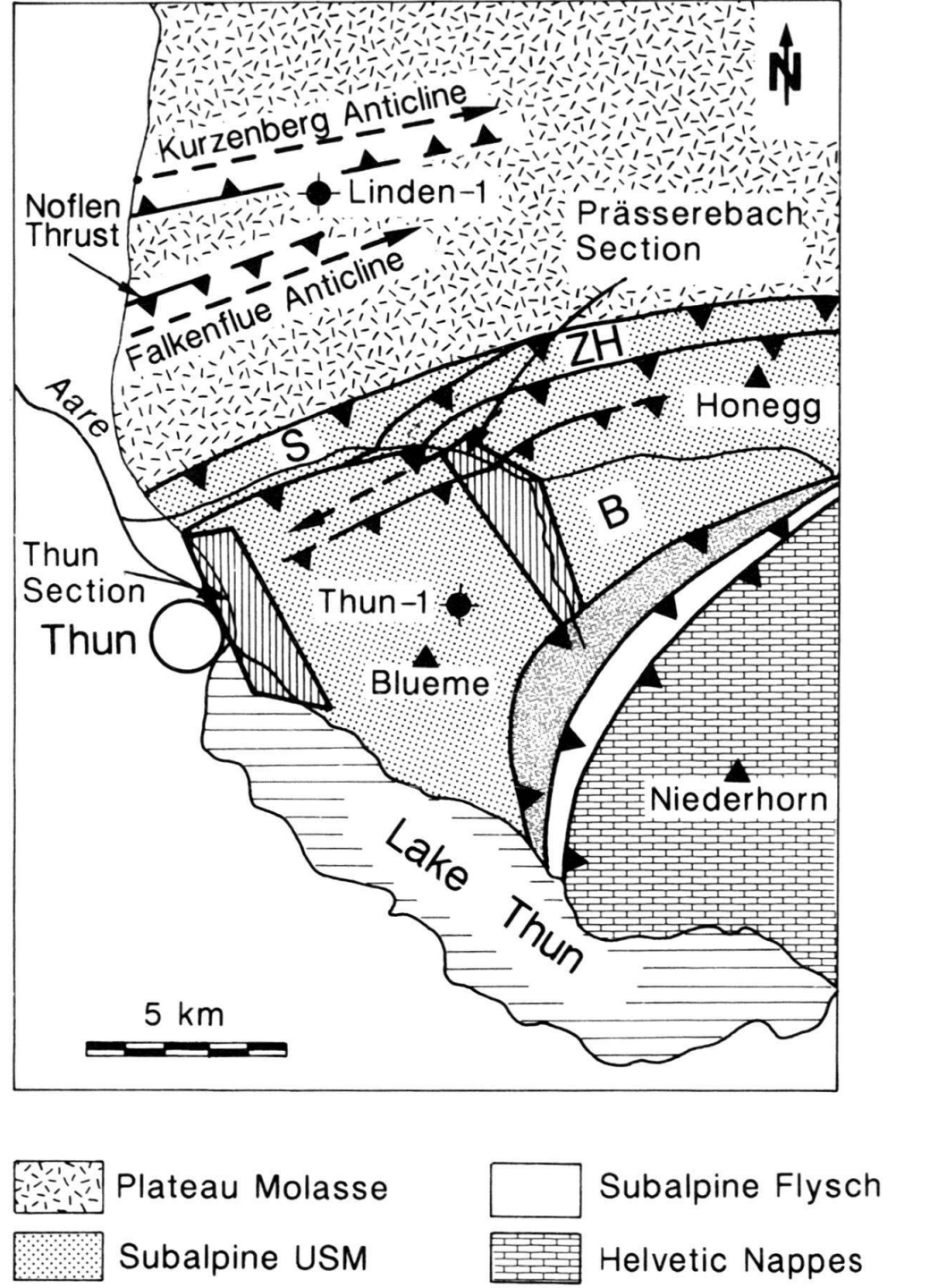
Petrographic modal analyses of sandstones were carried out on thin sections stained with alizarin red S and potassium ferricyanide to aid carbonate identification. A total of 300 points were analysed from each thin section using a Swift automatic point counter.

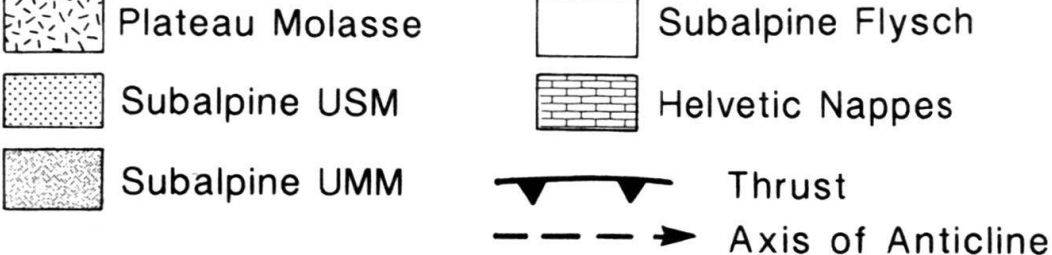
Heavy mineral analysis has proven to be a useful tool in the North Alpine Foreland Basin for reconstructing the sediment dispersal patterns, correlating sections and for unravelling the structure of the Subalpine Molasse (e.g. Füchtbauer 1964, Gasser 1968, Maurer 1983 and others). Some 53 heavy mineral analyses of sandstone samples from outcrops and 111 analyses of cuttings samples from the well Thun-1 were carried out. The samples were gently crushed with pestle and mortar and then left for 2 days in hot 10% acetic acid to dissolve the carbonate. The resulting sand was washed through a 60 μm sieve to remove the fine fraction and the remaining material was left to dry. From this sand the 400 to 60 µm size fraction was selected by sieving and the heavy minerals were separated from 10 to 20 grams of this material by centrifuging in bromoform. Modal analysis was made by counting 100 transparent grains. Opaque grains were not included in the counts, and garnet was counted separately. Authigenic anatase and brookite were also counted separately (for methodological details see Mange & Maurer 1992). The percentage of these three minerals is expressed relative to 100% transparent grains and therefore these percentages may themselves exceed 100%. The heavy mineral formula of Füchtbauer (1964) allows a brief characterisation of each heavy mineral facies or zone. Garnet is listed first in the formula, with capital G if it is the dominant sepcies, if not with a lower case g. The other minerals follow in the order of decreasing abundance. The major species (> 10%) are listed with a capital symbol, minor components (2-10%) with a lower case symbol. A = apatite, E = epidote, P = pyroxene, H = hornblende, S = staurolite, T = tourmaline and Z = zircon. In this study heavy mineral data from both outcrop and borehole samples are compared raising the question of intrastratal solution. The fact that epidote occurs in abundance even at 4000 m depth in the Thun-1 well confirms the results reported by Schlanke (1974) that intrastratal solution is negligible in the Swiss Molasse Basin. The heavy mineral data are given in Tables 2 and 3 (after the references).

For biostratigraphy, dark coloured silty marls with gastropods which are prone to contain micromammal teeth were sampled, dried and washed through a 0.5 µm sieve. The residue was studied under a binocular microscope and the micromammal teeth were hand-picked. Within the sections, several reference faunas of the biozonation of Engesser & Mayo (1987) were found. This mammal biozonation has been partly calibrated by magnetostratigraphy (Burbank et al. 1992). Faunal lists and biozones of the sites Schwändibach, Losenegg 2 and Prässerebach are given in Engesser (1990). A biostratigraphic discussion of the fauna, including new discoveries will be presented by Schlunegger (1994) together with the paleomagnetic data. In this paper the new time-scale for the late Cretaceous and Cenozoic by Cande & Kent (1992) is used.

3. Geological setting

The study area lies at the present alpine front to the east of Thun and comprises the southernmost Plateau Molasse and the Subalpine Molasse (Fig. 1). The sedimentary sequence of the Plateau Molasse in this region consists of Lower and Upper Freshwater Molasse, possibly without OMM in-between, ranging in age from Chattian to Langhian. The generally flat-lying Plateau Molasse has been affected by folding and by embryonic thrusts.





Steffisburg Thrust Sheet

ZH: Zulg-Hombach Thrust Sheet

Blueme Thrust Sheet

Fig. 2. Tectonic map of study area. Studied sections are shown in solid vertical hatching.

The Subalpine Molasse is made up of Lower Marine Molasse (UMM) and Lower Freshwater Molasse (USM) which occur in separate thrust sheets dipping steeply towards the SE underneath the Helvetic Nappes. The Subalpine USM is a complex unit comprising three thrust sheets: Steffisburg, Zulg-Hombach and Blueme thrust sheet (Fig. 2). These are overlain by the tectonically highest unit of the Subalpine Molasse thrust slices which is composed only of Lower Marine Molasse (UMM). According to Diem (1986) the UMM represents a continuous shallowing-upward sequence with turbidites passing upwards into coastal sandstones.

4. Stratigraphy

The most complete sequence of proximal USM in the Thun area with a thickness of more than 4500 m is preserved in the Blueme thrust sheet. The succession is well-exposed along the banks of high-gradient rivers such as the Prässerebach, and along the northern shore of Lake Thun (Fig. 2). It is divided into six informal units which are, in stratigraphic order: Homberg Beds/Schwändibach Conglomerate, Losenegg Beds, Thun Conglomerate, Honegg Marls and Gitzischöpf Conglomerate. A lithostratigraphic scheme with formal units of the entire Subalpine Molasse between Lake Thun and Rigi mountain will be presented in Schlunegger (1994).

These lithostratigraphic units are characterised by different litho- and petrofacies. The lithofacies are characteristic of alluvial fan and fluvial depositional environments (e.g. Steel et al. 1977, Heward 1978, Miall 1978, DeCelles et al. 1991, Platt & Keller 1992). The sequence ranges from the micromammal assemblage zone Oensingen to Brochene Fluh 53 (Engesser & Mayo 1987), i.e. it encompasses almost the entire Chattian (MP 26 to MP 30, Engesser 1990).

4.1 Schwändibach Conglomerate

The Schwändibach Conglomerate occurs in the southwestern part of the study area. The Thun section (Figs. 2, 3) reveals a 400 m thick succession of conglomerates typically consisting of 6 m thick massive clast-supported cobble-conglomerate sheets with shallow erosional bases, some with gutter casts. They tend to be moderately- to well-sorted, lack size grading and frequently show imbrication. Vertically stacked beds measuring 12–15 m occur frequently. The conglomerates are interbedded with 2–5 m thick units made up of alternating sandstones, siltstones and mudstones showing mottling, slickensides and root casts. Sandstones are subordinate and less than 1 m thick. They are commonly massive and more rarely normally or inversely graded with occasional ripples.

The petrofacies is characterised by a dominance of siliceous limestones clasts in the conglomerates, equal proportions of the different types of rock fragments in the sandstones, and a garnet-rich apatite-epidote-staurolite-tourmaline-zircon heavy mineral association, with either apatite or epidote as most abundant mineral (G, AESEZT association, see Tables 1, 2 and Fig. 3).

The Schwändibach Conglomerate is dated with a micromammal fauna representing the assemblage zone Oensingen (Engesser & Mayo 1987), i.e. earliest Chattian.

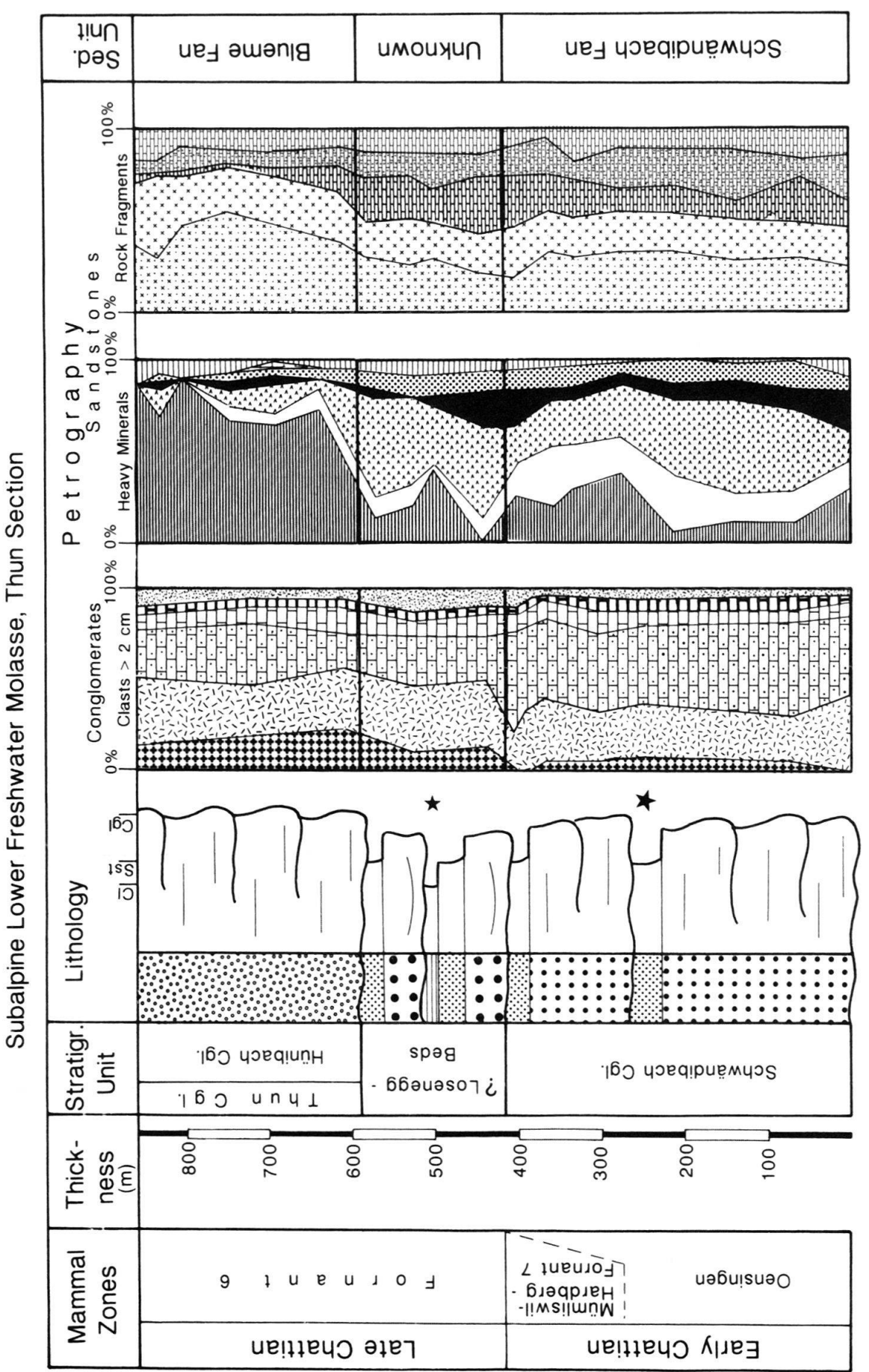


Fig. 3. Stratigraphy and sedimentary petrography of the subalpine Lower Freshwater Molasse of the Thun section. For location see Fig. 2 and for legend Fig. 9.

Interpretation

The lateral extent of individual beds cannot be recognised because of dense vegetation, which hinders the reconstruction of the depositional environments. The shallow erosional bases in association with the unstratified and ungraded nature and imbrication of the conglomerates, however, suggests deposition on longitudinal gravel bars in braided channels on an alluvial fan. The considerable thickness of both single and amalgamated conglomerate bodies probably indicates fairly high channel stability. The associated fine grained deposits are interpreted as overbank fines on the basis of their grain size and abundance of pedogenetic phenomena. They were laid down on flats in-between braided channel belts.

4.2 Homberg Beds

The Homberg Beds are a fine-grained unit lacking conglomerates which crops out at the base of the Prässerebach section (Fig. 4). A micromammal fauna found near the base of this section is within the Oensingen assemblage zone (Engesser & Mayo 1987). Hence, the Homberg Beds are partly coeval with the Schwändibach Conglomerate. Both units are in tectonic contact with the Steffisburg thrust sheet.

The Homberg Beds, with an exposed thickness of approx. 500 m, consist mainly of different sandstone facies and intercalated thinner siltstone and mudstone units. Laterally extensive medium grained sandstones occur as 2–8 m thick simple bodies or as up to 15 m thick amalgamated packages. The sandstones have erosive bases lined with mudstone pebble lags. They form fining-upward cycles with low-angle "epsilon" crossbedding, trough cross-bedding followed by ripple cross-lamination and, near the top, by climbing ripple-lamination. Mottling and bioturbation increase towards the top of the cycles.

Fine to medium grained sanstones are found as less than 2 m thick and 20 m wide lenticular channel bodies with erosional bases. They are commonly weakly graded, massive or trough cross-bedded with bioturbated and mottled tops. They occur in association with thin (< 1 m) laterally continuous fine grained sandstone sheets displaying sharp basal contacts and normal or inverse grading.

Fine grained deposits measuring 1-20 m in thickness occur interbedded with the sandstones. They consist of alternating thinly bedded siltstones and mudstones. The siltstones show convolutions as well as ripple and climbing ripple cross-lamination, the mudstones are weakly laminated. These fine grained sediments are further characterised by strong brown and yellow mottling, slickensides and bioturbation.

The medium grained sandstones of the Homberg Beds classify as feldspathic litharenites in a McBride (1963) triangular plot. The different types of rock fragments occur in approximately equal proportions (Fig. 4). The heavy mineral suite is dominated by garnet and apatite associated with abundant tourmaline and lesser amounts of staurolite, epidote and zircon (G, ATsez heavy mineral association, Table 2).

Interpretation

Similar lithofacies to the Homberg Beds have been described by Platt & Keller (1992) from the distal USM. The medium grained sandstones represent channel deposits which

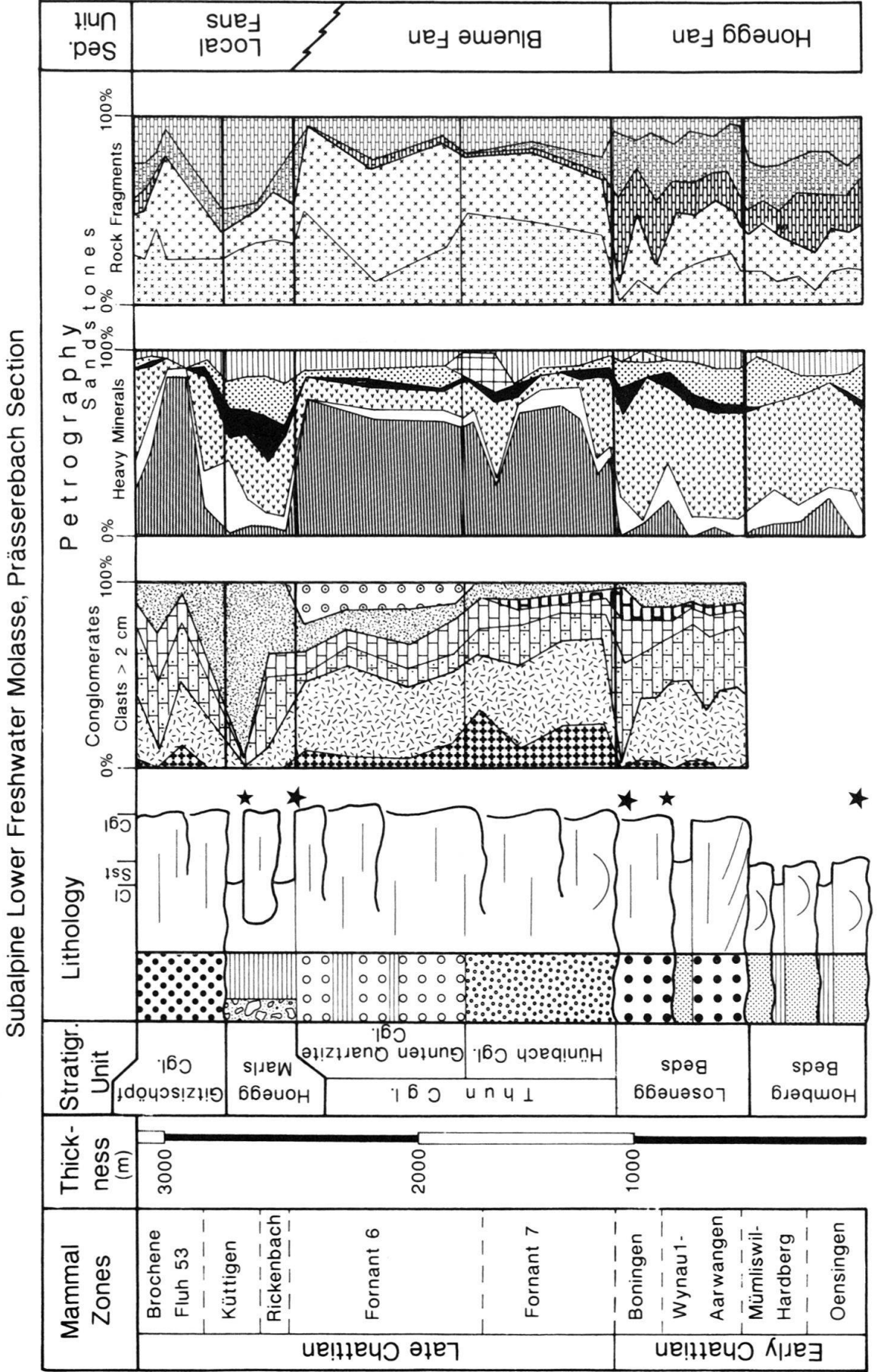


Fig. 4. Stratigraphy and sedimentary petrography of the subalpine Lower Freshwater Molasse of the Prässerebach section. For location see Fig. 2 and for legend Fig. 9.

were laid down by lateral channel migration as indicated by the epsilon cross-beds and the associated grooves and imbricated pebble lags revealing a flow direction perpendicular to the dip azimuth of the lateral accretion surfaces. The association of (a) fine to medium grained sandstones with lenticular geometry and smaller thickness with (b) sandstone sheets is interpreted as crevasse channels and splays. The fine-grained sediment packages represent the levee and floodbasin deposits of Platt & Keller (1992). These sediments were strongly modified by bioturbation and pedogenetic processes during longer periods of subaerial exposure, although no redbeds developed.

4.3 Losenegg Beds

The Losenegg Beds, with a thickness of 450 m, rest with a sharp contact upon the Schwändibach Conglomerate in the area northeast of Thun, or upon Homberg Beds further to the east (Fig. 5). The Losenegg Beds are composed of fining upward sequences beginning with conglomerates. Individual conglomerates measuring 2–20 m occur as laterally continuous (100's of m) single or amalgamated units. The conglomerates, which account for 60% of the total thickness, have deeply scoured (1–1.5 m) erosional bases with strongly concave shape, many marked by gutter casts. The clast-supported cobble-conglomerates are well-rounded and well-sorted. They are commonly unstratified but contain numerous cross-bedded sandstone lenses. More rarely, low-angle "epsilon" cross-beds are present which dip at right angles to the gutter casts. The average maximum clast size increases from about 10 cm at the base to about 20 cm at the top of the unit. The conglomerates are generally followed by 0.2–2 m thick fining-upwards sandstones topped by siltstones and mudstones. These fine grained sediments display plane-lamination, ripple cross-bedding, mottling, root traces and bioturbation. However, massive beds are common due to pedogenic and biogenic destratification.

Conglomerate clast counts of the Losenegg Beds reveal 40-50% igneous and metamorphic and 25-40% siliceous limestone clasts. The remainder are limestones, dolomites and sandstones which occur in more or less equal amounts (Table 1). A few conglomerate beds found in the upper part of the sequence have a different clast composition characterised by an almost total absence of crystalline clasts. This difference is mirrored by the rock fragment composition of the associated inverse-graded sandstones as shown in Figure 4. The sandstones are feldspathic litharenites (classification of McBride 1963). They contain a garnet-apatite-tourmaline-staurolite heavy mineral association with lesser amounts of epidote and zircon (G, ATSez). Garnet and apatite are dominant with on the average 476% and 54% respectively (Table 2).

In the Prässerebach section the Losenegg Beds contain faunas of the micromammal assemblage zones Wynau 1 and Boningen corresponding to the late Early Chattian (Fig. 4) whereas a fauna found in the Thun section gives a maximum age of Fornant 6 (Fig. 3). Although in the Thun section this unit has identical lithological and petrographic characteristics with the Losenegg Beds of the Prässerebach section, its younger age and spatial separation (Fig. 5) suggest that it may correlate with a lithostratigraphic unit to the west of the Aare valley.

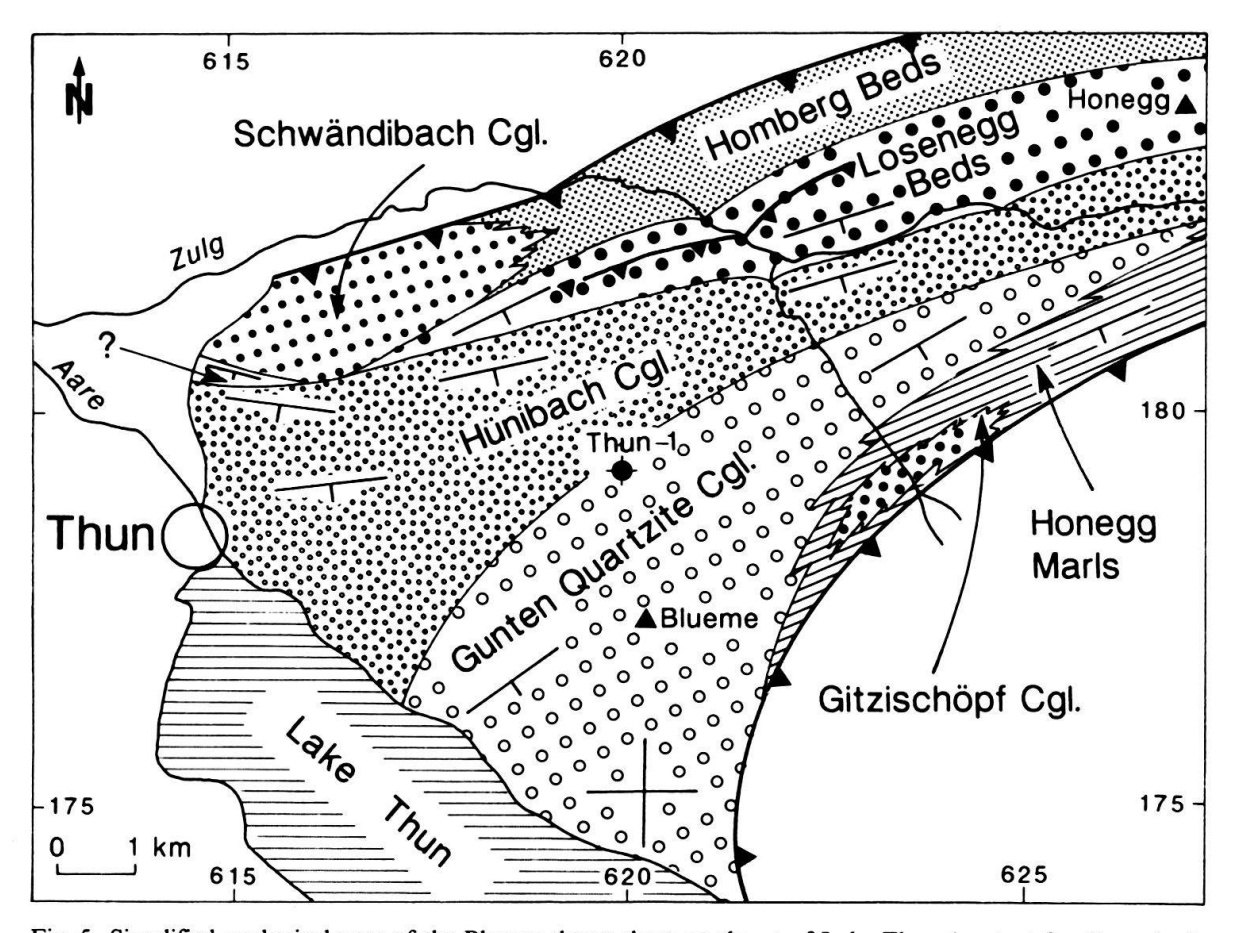


Fig. 5. Simplified geological map of the Blueme thrust sheet northeast of Lake Thun (see text for discussion).

Interpretation

The erosional concave bases, clast-supported framework, good sorting and crude upward fining of the conglomerate beds indicate deposition in fluvial channels. The presence of epsilon cross-bedding resulted from lateral accretion, probably on side bars in sinuous channels, whereas the predominantly unstratified nature and the occurrence of numerous sandstone lenses within the conglomerates suggest deposition on longitudinal bars and fluctuating water stages. The fining upward fine grained units capping the conglomerate beds comprise rippled sandstones deposited during waning floods in channels as well as overbank facies overprinted by pedogenesis.

4.4 Thun Conglomerate

The Thun Conglomerate consisting of over 1300 m of mainly polymict cobble to boulder conglomerates has been divided into the Hünibach Conglomerate and Gunten Quartzite Conglomerate (Fig. 4). The Hünibach Conglomerate measuring 550 m in the Prässerebach section comprises single (4–6 m) and amalgamated (> 10 m) conglomerate bodies and intercalated fine-grained units. Conglomerates make up for 90% of the total thickness of this member. The well-rounded clast-supported cobble conglomerates commonly have an erosional lower bounding surface with gutter casts and pebble lag. Some

beds are unstratified, others show tabular or trough cross-bedding, horizontal stratification, imbrication and a weak fining-upward trend. The conglomerate bed thickness was observed to increase upsection. The interbedded fine grained units measuring 5-10 m comprise coarse to fine sandstones, rippled siltstones and mottled reddish mudstones in fining upward sequences.

The Gunten Quartzite Conglomerate measures more than 800 m in the Prässerebach section. It consists mainly of well-rounded clast-supported cobble-conglomerates which comprise about 95% of the member. They form amalgamated units 10's of m in thickness which are made up of 0.5-2 m thick beds that wedge out laterally. Individual beds within the amalgamated units are easy to recognise because of the appearance of thin cross-bedded sandstones at the top of each bed. The conglomerate beds are erosively-based and commonly unstratified, although horizontal stratification and clast imbrication are occasionally developed. The thickness of the conglomerate units decreases upwards as intercalations of yellow siltstones and mudstones become more abundant, making a gradual transition to the overlying Honeg Marls. The upper boundary of the Gunten Quartzite Conglomerate is arbitrarily drawn at the level where the yellow marls occupy more than 50% of the succession.

The petrofacies of the Hünibach Conglomerate is characterised by a high amount (55-75%) of metamorphic and igneous clasts, particularly red granite. In addition to a high proportion of crystalline rocks, the Gunten Quartzite Conglomerate contains abundant clasts of quartzites from the greenschist facies and is lacking dolomite cobbles (Table 1). Similarly, more than 80% of the rock fragments in the sandstones of both members which classify as litharenites are derived from crystalline rocks. The heavy mineral association of these sandstones is dominated by garnet and epidote which are accompanied by about 15% apatite and small amounts of staurolite, tourmaline and zircon (G, EAstz) as shown on Table 2 and Figures 3 and 4.

The age of the Thun Conglomerate is determined by micromammal faunas found in the adjacent stratigraphic units. These faunas suggest an early Late Chattian age for the Prässerebach section and a slightly younger age for the Thun section (Figs. 3, 4).

Interpretation

The predominantly conglomeratic succession displays the features described from gravelly braided streams (e.g. Rust 1978, Miall 1978, 1985). The generally shallow erosive bases with pebble lags, clast-supported framework and crude upward fining suggest deposition of the conglomerates in channels. The association of unstratified, imbricated and cross-bedded conglomerates characteristic of the Hünibach Conglomerate member indicates deposition on longitudinal bars and the intervening channels (Smith 1974, DeCelles et al. 1991). In comparison to the Hünibach Conglomerate, the higher proportion of conglomerates, their more pronounced lenticular shape, unstratified nature and thinner bed thickness in the Gunten Quartzite Conglomerate indicate a more intricate braided pattern and shallower channels and thus a more proximal depositional environment.

4.5 Honegg Marls

The Honegg Marls measure more than 240 m in the Prässerebach section (Fig. 4). They consist of $\sim 70\,\%$ marls interbedded with thin sandstones ($\sim 20\,\%$) and a few conglomerates. The marls are either massive, massive with scattered pebbles, or dm-bedded and graded. Individual marl beds often show a decreasing iron oxydation state towards the top. Black mudstones with a thickness of $10-50\,\mathrm{cm}$ and a scarce fauna and flora including gastropods and and the fruits of Celtis sp. are also present. The well-rounded and moderately sorted cobble- to boulder-conglomerates are less than 3 m thick and pinch out laterally within a few meters. Vertical stacking of $2-5\,\mathrm{beds}$ leads to $12-15\,\mathrm{m}$ thick conglomerate bodies of limited lateral extent. The clast-supported conglomerates may be either unstratified or cross-bedded. Moreover, thin $(20-50\,\mathrm{cm})$ and only $2-3\,\mathrm{m}$ wide pebble-conglomerate lenses with weakly erosional bases and invers grading occur scattered in the marly background sediment. Similarly, the sandstones generally measure a few centimeters in thickness and can be traced laterally only over a few meters.

Conglomerate clast counts reveal a strikingly high percentage of sandstone clasts derived from the alpine Flysch units (Table 1, Fig. 4). In the sandstones rock fragments of crystalline and sedimentary origin are equally abundant. The heavy mineral suite (Table 2) is characterised by high garnet and low epidote percentage and equal amounts of apatite, staurolite, zircon and tourmaline (G, ASTZe-association).

A micromammal fauna from the base of the Honegg Marls indicates assemblage zone Fornant 6, whereas another fauna from higher in the section gives a less precise age, from Rickenbach to Boudry 2 (Fig. 4). Together, these faunas suggest a Late Chattian age of the Honegg Marls from the top of Fornant 6 to possibly Küttigen (Fig. 4).

Interpretation

The conglomerates cutting deeply into the mudstones and forming vertically stacked packages obviously filled narrow channels which occupied stable positions over prolonged periods. The lack of pebble lags, moderate sorting, rare stratification and the presence of outsized clasts suggest deposition by major high-concentration floods. However, the absence of a fine-grained matrix and the clast-supported framework suggest that the principal transport mechanism was a hyperconcentrated flow (Pierson 1980) rather than a pseudoplastic debris flow. The deep longitudinal furrows are an indication for turbulent flows. Beyond the intersection point sheet floods developed and deposited thin inversely graded conglomerate sheets in very shallow braided channel courses on the lower muddy reaches of the fan. The fine-grained background sediment documents a wide range of depositional processes within a floodplain environment, from mudflows depositing marls with scattered pebbles to sheetfloods leading to laminated mudstones and rippled sand- and siltstones. The immature soil profiles which developed on these sediments and the occurrence of black mudstones, interpreted as swamp deposits, indicate a high aggradation rate on a wet muddy floodplain.

4.6 Gitzischöpf Conglomerate

The Gitzischöpf Conglomerate occurs at the top of the USM in the study area. Its present thickness of 250 m does not represent the true depositional value because the sequence is truncated at the top by the basal thrust of the overlying UMM. The Gitzischöpf Conglomerate is composed of a conglomerate and a silty mudstone facies. The conglomerate occurs as < 6 m thick bodies with concave-up erosively-based contacts and convex-up upper surfaces. These lensoid bodies wedge out laterally over 300-100 m. The clast-supported cobble-conglomerates are well-rounded and moderately- to well-sorted. Clast size varies up to 25 + cm and the average clast size is 8-10 cm. They are either unstratified or show horizontal stratification. Clast imbrication is common. The red silty mudstones generally display red and yellow mottles and calcrete glaebules which is characteristic of stage-1 soils (entisoils) described by Bown & Kraus (1987). More rarely they are plane-laminated and rippled.

Petrographic analyses document frequent compositional changes during deposition of the conglomerates and sandstones (Table 1, Fig. 4). The heavy mineral composition varies from an epidote to an apatite dominated suite (Table 2). This change goes in parallel with high vs. low amount of crystalline components in the conglomerates and sandstones. No datable fossils were recovered, and therefore dating of the Gitzischöpf Conglomerate must await the results of ongoing palaeomagnetic studies.

Interpretation

Because of their lens-like shape, the presence of erosional surfaces and their stratified nature, the conglomerates probably resulted from streamflow deposition on gravel bars in small braided channels. The silty mudstones were deposited by mudflows and muddy streamflows and subsequently modified by pedogenetic processes. The presence of entisoils which are interpreted by Bown & Kraus (1987) as immature soils points to high aggradation rates. The small size of the channels combined with the frequent, abrupt petrofacies changes is taken as evidence for interfingering of two local fans draining different source terrains.

5. Depositional systems

The different lithofacies of the USM can be accounted for by deposition from streamflow, hyperconcentrated flows and pseudoplastic debris flows on alluvial systems. The distribution of the lithofacies and the petrofacies in space and time reveals three major and two local alluvial fan systems (Figs. 5, 6).

The first major alluvial system consists of the Schwändibach Conglomerate and is referred to as the Schwändibach fan. Its depocentre which is documented by a predominance of conglomerates and coarse clast sizes is located a few kilometers to the NE of Thun (Figs. 5, 6). Further northeastwards, the decreasing number of conglomerate beds and clast size mark the facies change from the Schwändibach Conglomerate to the Homberg Beds.

The second major depocentre crops out in the chain of hills with Honegg as a summit. It is composed of the Homberg Beds and the Losenegg Beds and represents the Honegg

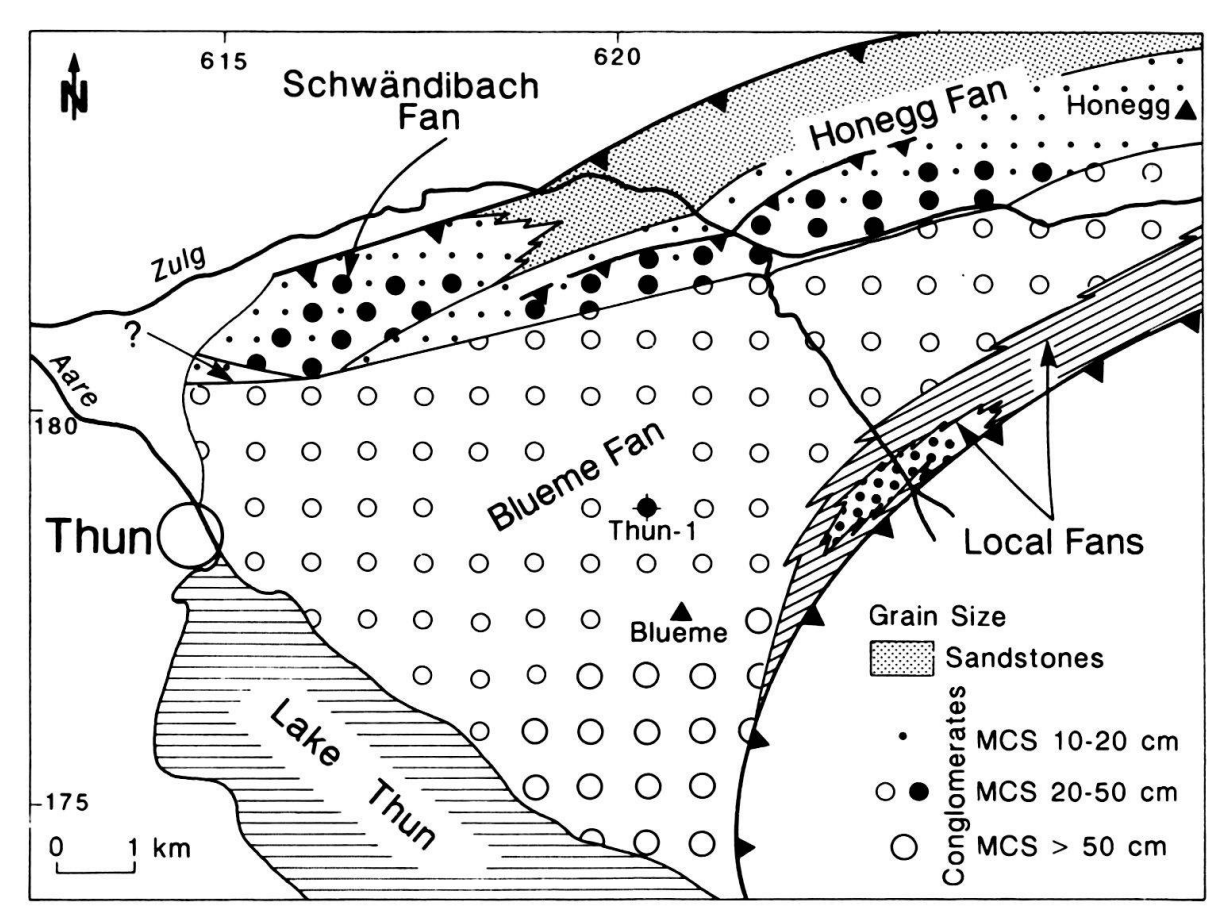


Fig. 6. Map showing alluvial fan systems of the Lower Freshwater Molasse of the Blueme thrust sheet northeast of Lake Thun. Note coarsening upward trends of Schwändibach, Honegg and Blueme alluvial fans.

fan (Figs. 5, 6). This fan is characterised by a mixture of crystalline and sedimentary clasts and by a G, ATsez heavy mineral association. Although the petrofacies of the Honegg fan and the Schwändibach fan are similar they differ with regards to the amount of crystalline clasts and the percentage of apatite, epidote and staurolite (Figs. 3, 4). Progradation of the Honegg fan is recognizable from the coarsening upward trend associated with a change in fluvial style from meandering (Homberg Beds) to sinuous (Losenegg Beds).

A very different petrofacies with a predominance of crystalline components in the conglomerates and sandstones and a heavy mineral association dominated by epidote characterises the third major alluvial fan referred to as Blueme fan. The thickness of the alluvial sediments comprising the Hünibach and the Gunten Quartzite Conglomerate increases from >1300 m in the Prässerebach section to >4000 m in the Lake Thun section (Figs. 5, 6). Moreover, maximum clast size also increases from 10-20 cm at the base of the section near Thun to >1 m in fanhead deposits at its top (Beck 1911). The upward coarsening associated with the tendency towards a more intricately braided style and shallower channels indicate progradation of the Blueme fan. Despite the different composition of the conglomerates the Hünibach and Gunten Quartzite Conglomerate represent one single fan as revealed by the parellelism of the lateral thickness changes, identical composition of the sandstones and the progradational habit.

The Honegg Marls and the Gitzischöpf Conglomerate represent at least two separate fans judging from the different petrofacies and the onlap relationships with the Blueme fan (see below). The small fan size in the case of the Gitzischöpf Conglomerate, in combination with small channel size, abundant mass flows and abrupt compositional changes taken together suggest a local origin of these fans. However, an alternate interpretation of the Honegg Marls as a bajada, rather than a single fan cannot be ruled out at present.

Mapping of these alluvial systems enabled their geometrical relationships to be reconstructed. The converging strike directions of the bedding of Hünibach Conglomerate and Losenegg Beds shown in Figure 5 indicate a structural discordance, with Losenegg Beds missing as in the Thun borehole (Fig. 8). Figure 7 shows that this erosional hiatus increases southwestwards with the entire Honegg fan missing in the Thun section. The position above the unconformity of the ?Losenegg Beds in this section indicates that this unit is part of another fan system whose depocentre lies west of the

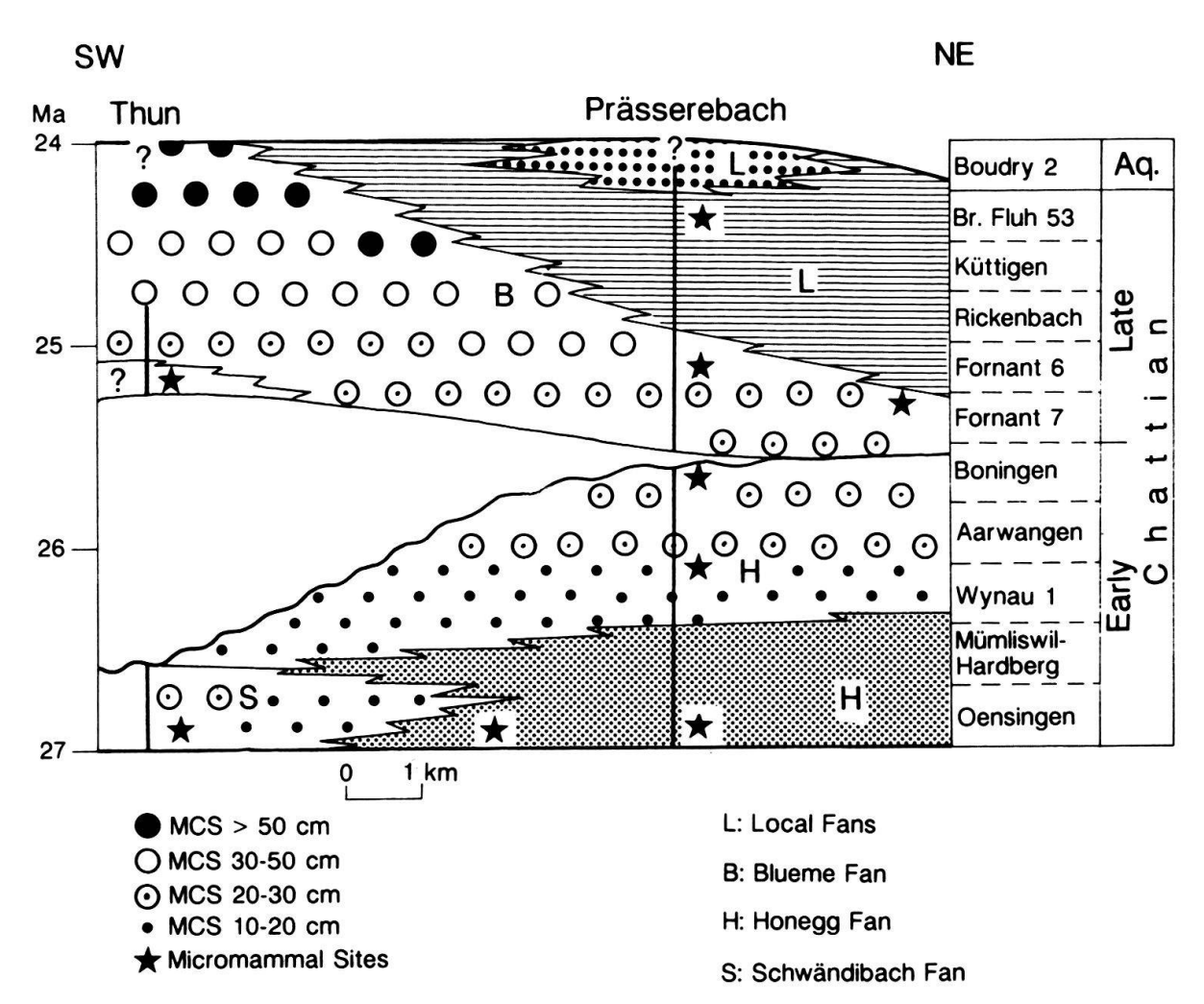


Fig. 7. Chronostratigraphic (Wheeler) diagram of the Blueme thrust sheet based on micromammal biostratigraphy, calibrated by paleomagnetics after Burbank et. al. (1992) and Schlunegger (unpubl. data). Strike parallel section. Note heterochroneity of alluvial fans, erosional hiatus and migration of Blueme fan axis indicated by lateral shift of maximum clast size (MCS) through time.

Aare valley. It is also evident from Figure 7 that the base of the Blueme fan is heterochronous and the fan axis shifts from NE to NW.

Divergent strike directions of the beds in the Hünibach and Gunten Quartzite Conglomerate and the smaller size of the upper part of the fan represented by the younger member are explained by progradation of the Blueme fan. At a given cross-section the width of the fan decreases, whereas the gradient increases as the fan progrades. This together with the shift of the fan axis explains the observed lateral onlap of the local fan on the Blueme fan: from northeast to southwest the Honegg Marls interfinger first with Hünibach Conglomerate and then with progressively younger beds of the Gunten Quartzite Conglomerate (Fig. 5).

6. Structure

In this section, the structure of the southern margin of the Molasse basin and the stratigraphic correlation of Subalpine and Plateau Molasse will be discussed using outcrop, borehole and seismic data. The gas wells Linden-1 and Thun-1 both penetrated the entire Molasse sequence.

The Thun-1 borehole located in the Subalpine Molasse (Fig. 2) drilled 5151 m of USM which rests upon Eocene "sidérolithique" with UMM missing (Micholet 1992).

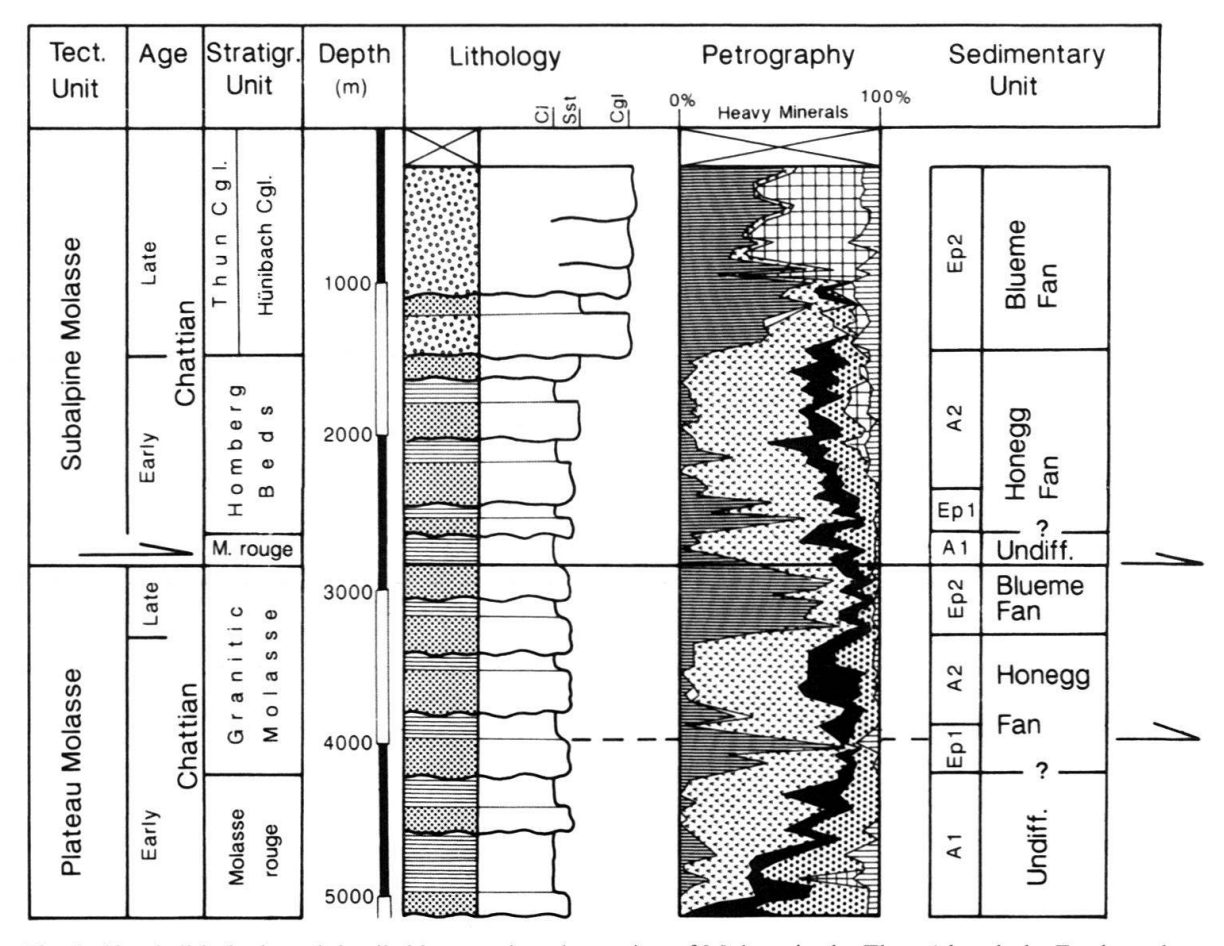


Fig. 8. Simple lithologic and detailed heavy mineral zonation of Molasse in the Thun-1 borehole. For legend see Fig. 9.

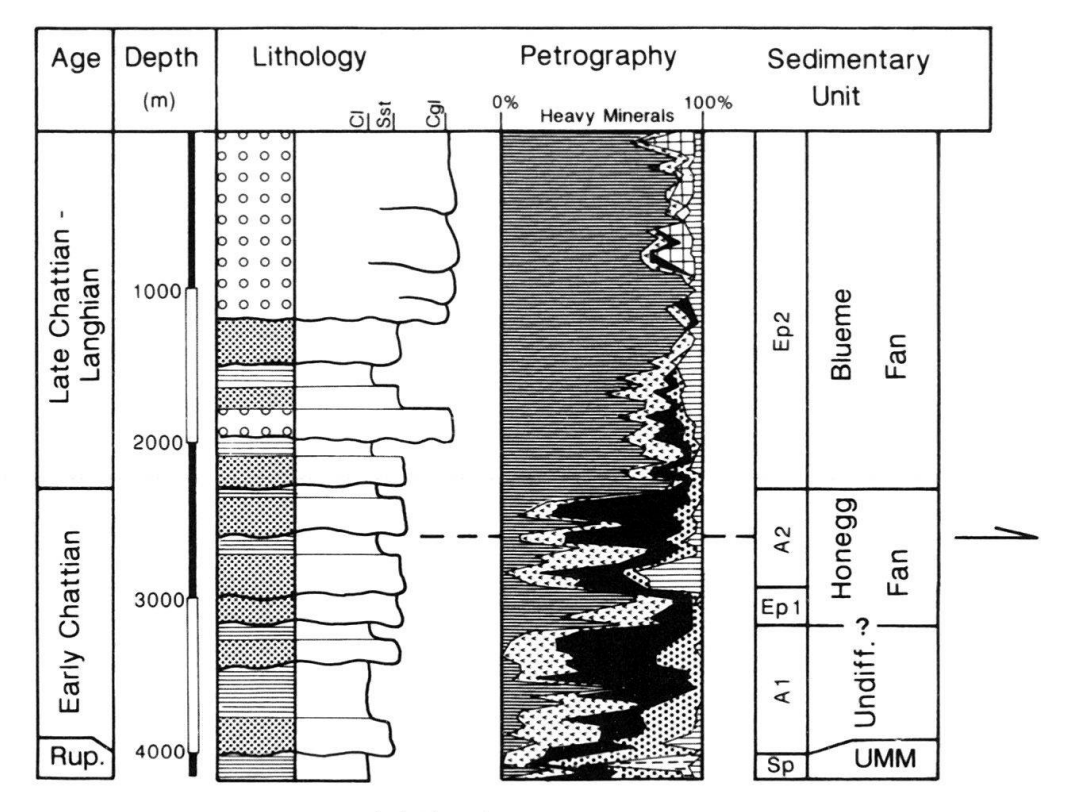
Based on closely spaced heavy mineral analyses (Table 3) the section is divided in eight heavy mineral zones as shown on Figure 8. The heavy mineral zonation enables the overthrust of the Subalpine Molasse to be precisely located at 2940 m. Furthermore, the heavy mineral zones A 2 (apatite-rich) and Ep 2 (epidote-rich) of the borehole can be correlated with the Homberg Beds and Hünibach Conglomerate at the surface on the basis of their characteristic heavy mineral suites. Note that pyroxene and hornblende also occur in the borehole at the same stratigraphic position as in the outcrop section, though in different percentages (Figs. 4, 8). The Losenegg Beds are missing in the borehole as pointed out further above which indicates an erosional unconformity at the top of the Honegg fan. At the base of the Subalpine Molasse another epidote-rich (Ep 1) and an apatite-rich unit (A 1) are found which however, do not crop out at the surface.

These four heavy mineral zones are repeated in the autochthonous Molasse beneath the Blueme thrust sheet (Fig. 8). Compared to the Subalpine Molasse, the zones Ep 2 and A2 in the authochthonous sequence are finer grained. Mudstones occupy a greater thickness of the section, and conglomerates are lacking. The autochthonous section of the Thun-1 well represents a more distal facies of the Blueme and Honegg fans. It contains sandstones rich in feldspar, characteristic of the so called Granitic Molasse (Habicht 1987, p. 120). The lithology of the heavy mineral zone A1 consists of an alternation of thin sandstones with red mudstones. It is interpreted as Molasse rouge. Lacking detailed lithological information and without access to electrical logs, however, no sedimentological interpretation of the Molasse rouge is possible at present. Judging from the heavy minerals alone the Molasse rouge might represent a distal facies of the Honegg fan. The lower part of the USM, characterised by an apatite rich heavy mineral facies (incl. Ep1), was interpreted by Maurer et al. (1978) as sourced from a single dispersal system, called the Lütschine dispersal system. The epidote rich facies typical of the Blueme and Napt fan was attributed to the Thunersee dispersal system.

The Linden-1 borehole is located in the Plateau Molasse at approximately 11 km distance from Thun-1. The heavy minerals show the same mineral zones as in the Thun-1 well, except for a chromian spinell association at the base of the sequence (Fig. 9). This lowest heavy mineral zone is interpreted as UMM based on the presence of spinel, a marine microfauna and calareous nannoplankton indicating a Rupelian age (Zimmermann et al. 1976). The upper part of zone Ep2 are conglomerates which according to Maurer et al. (1978) represent a terrestrial facies of the OMM of Burdigalian-Langhian age, i.e. Upper Freshwater Molasse. However, zone Ep2 correlates with the Late Chattian Thun Conglomerate in the well Thun-1 and in the outcrops of the Subalpine Molasse, which indicates considerable progradation of the Blueme fan.

Figure 10 a shows a hand line drawing of an unmigrated seismic section which extends from the southern edge of the Plateau Molasse across the Subalpine Molasse. This section passes over the borehole location of Linden-1 and Thun-1, allowing interpretation of the lithologies of the reflectors and correlation of the lithologic units of Plateau and Subalpine Molasse. The same seismic section was recently published and interpreted by Vollmayr (1992).

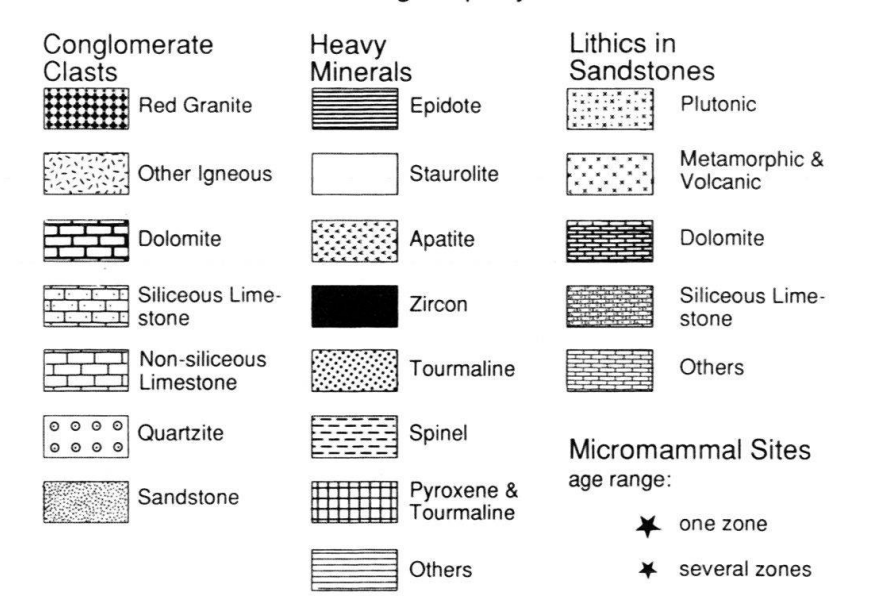
The top of the Mesozoic is located at 4350 m in Linden-1 (Maurer et al. 1978) and 5203 m in Thun-1 (Micholet 1992), demonstrating that the karstified surface of the Mesozoic dips gently southwards. Strong reflectors originate from the top of the partly evaporitic Triassic and the Malm whereas the reflector marking the top of the basement



Lithology



Petrography



and what is interpreted as Permo-Carboniferous is less pronounced, indicating less impedance contrast of this boundary. The Molasse sequence is highly reflective, although many reflectors are discontinuous due to the limited lateral extent of the beds, particularly in the conglomeratic units.

Structural interpretation of the Thun Molasse

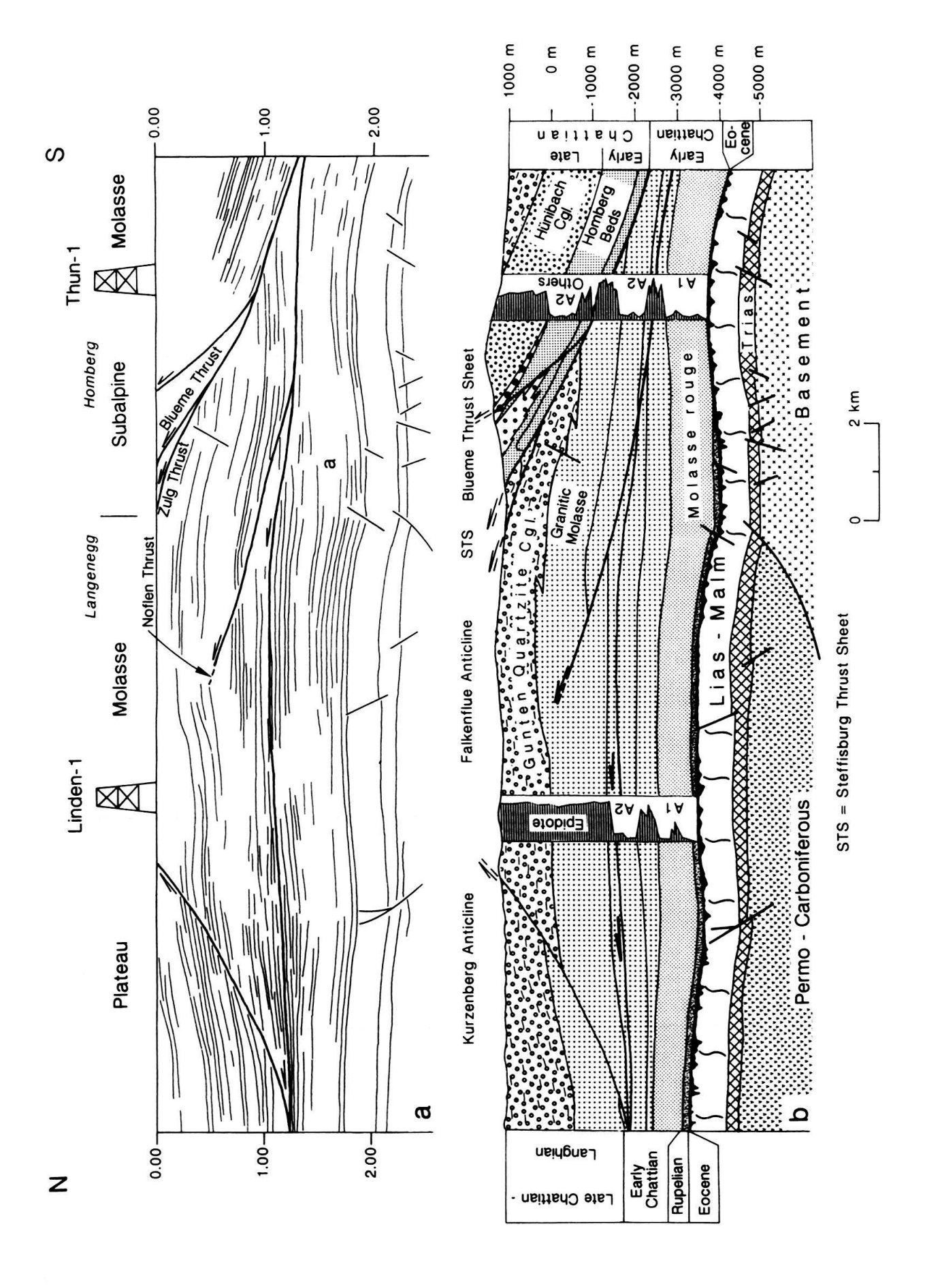
The reflectors shown on Figure 10a, in combination with outcrop and well data, permit a structural interpretation of the Thun Molasse (Fig. 10b). The abrupt change in the dip directions at the southern end of the seismic section coincides with steep dips at the surface marking the boundary of the Subalpine Molasse imbricate thrust stack and the Plateau Molasse. The close similarity of the facies in the Steffisburg thrust slice and adjacent Plateau Molasse suggests that the largest displacement occurred along the Blueme thrust fault rather than along the Zulg thrust fault as assumed by Micholet (1992). The Steffisburg thrust sheet is seen to be a small tectonic sliver compared to the Blueme thrust sheet (Fig. 10b).

The basal thrust of the Subalpine Molasse located in the Thun-1 borehole at 2940 m is recognisable on the seismic section from diverging dips and abrupt terminations of reflectors (Fig. 10a). Within the authochthonous Molasse, onlap reflections (a) in Figure 10a coincide with the base of the Honegg fan. This relationship suggests that some deformation had affected the Molasse rouge prior to the build-up of the Honegg fan.

The main structural features of the Plateau Molasse in the study area are the anticlinal structures of the Falkenflue and Kurzenberg together with the eastern prolongation of the Noflen thrust (Figs. 2, 10). In the Aare valley cross-section the Falkenflue anticline shows a flat southern limb and a steeper northern limb. Farther eastwards the anticline becomes more symmetrical and then dies out. The origin of this anticline is related to the Noflen thrust which it progressively replaces east of the Aare valley. This thrust ends blind in the core of the anticline, thus suggesting fault-propagation fold kinematics. The Kurzenberg anticline on the other hand resulted from southward thrusting of the Plateau Molasse along a north-dipping thrust fault (Fig. 10). As recognised by Vollmayr (1992), this gives rise to a triangle zone.

There is no clear-cut division of Plateau and Subalpine Molasse in the study area, neither in terms of geometry nor kinematics of deformation. According to Vollmayr (1992) the triangle zone (i.e. the Noflen thrust, Fig. 10a) represents this boundary. However, it is more aptly placed at the Blueme thrust where the most abrupt lithological change is observed and along which the largest displacement took place. In fact, rather than a sharp contact of Plateau and Subalpine Molasse the structural situation shown on Figure 10 reveals a transition which reflects the kinematics of deformation. All of the thrusts shown on Figure 10 are rooted in the major detachment horizon located within the USM implying a close kinematic relationship. The angle of dip of the thrust faults increases from north to south as a result of in-sequence tectonics by thrust fault propagation towards the foreland causing uplift and steepening of the overlying beds, as pointed out by Butler (1989) and Stäuble and Pfiffner (1991).

Fig. 9. Simple lithologic and detailed heavy mineral zonation of Plateau Molasse in the Linden-1 borehole (after Maurer et al. 1978, mod.) and legend to Figs. 3, 4, 8 and 9.



Using the top of the heavy mineral zone Ep1 as a reference horizon the shortening for the section shown on Figure 10 can be estimated. For the Subalpine Molasse it is about 8 km and 1 km each for the Falkenflue and Kurzenberg anticline.

7. Discussion

The cross-section through the Subalpine Molasse thrust stack and adjacent Plateau Molasse permits the structural restoration of the individual tectonic units and reconstruction of the sedimentological evolution of the Lower Freshwater Molasse in space and time. This evolution records the development of the basin/thrust wedge system through time, as pointed out by Sinclair et al. (1991) as well as the tectonic and the unroofing history of the Alps.

The structural restoration of the studied sections shown in Figure 11 reveals strongly heterochronous facies relationships at the southern margin of the Molasse Basin. This is the result of large-scale fan progradation beginning with the small Honegg fan and followed by the Blueme fan. The latter is not only much larger but it also prograded more rapidly. Furthermore, based on the heavy mineral assemblages the Granitic Molasse in the studied sector of the Swiss Plateau represents a more distal facies of the Honegg and the Blueme fan. Maurer et al. (1982) attributed the lower garnet and apatite-rich heavy

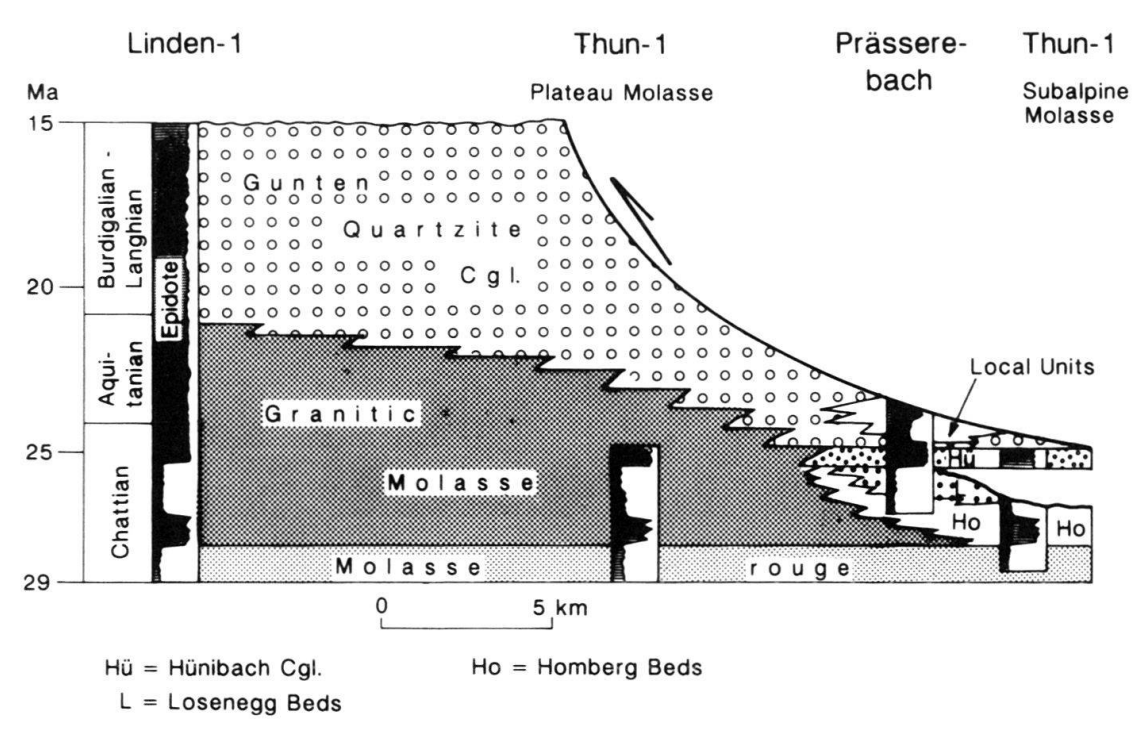


Fig. 11. Chronostratigraphic (Wheeler) diagram showing facies relationships of the terrestrial Molasse at the southern basin margin, northeast of Lake Thun. Diagram is based on a structural restoration of the thrust sheets of the Subalpine Molasse.

Fig. 10. Hand line drawing of unmigrated seismic section (a), and geological interpretation based mainly on heavy mineral correlation of outcrop and well sections (b). Only major thrust faults are shown (for comparison see fig. 2 in Vollmayr 1992).

mineral facies to the Lütschine and the upper epidote-rich facies to the Thunersee/Napf dispersal systems respectively.

The marked compositional change from the Honegg fan, dominated by sedimentary clasts and an apatite-zircon heavy mineral suite, to the Blueme fan, rich in igneous clasts and an epidote-rich heavy mineral assemblage, coincides with an erosional unconformity at the Early/Late Chattian boundary, at approximately 25 Ma. Based on previous studies on the origin of conglomerate clast types by Speck (1954), Trümpy & Bersier (1954), Matter (1964) and Gasser (1968) it is concluded that the detritus in the Honegg fan was derived from lower Penninic nappes whereas the igneous clasts indicate erosion of the structurally higher upper Penninic and Austroalpine nappes. Normally, unroofing of a nappe stack should lead to an inverse sequence in the foreland with the detritus from the highest units being eroded and laid down first, as is the case in the Southalpine Molasse (Giger 1991).

In Early Chattian time, the Penninic and Austroalpine nappe edifice had already been emplaced (Burkhard 1988). Also, the catchment area of the rivers feeding the Schwändibach and Honegg fans lay in the lower Penninic Prealpine nappes. Erosion of these

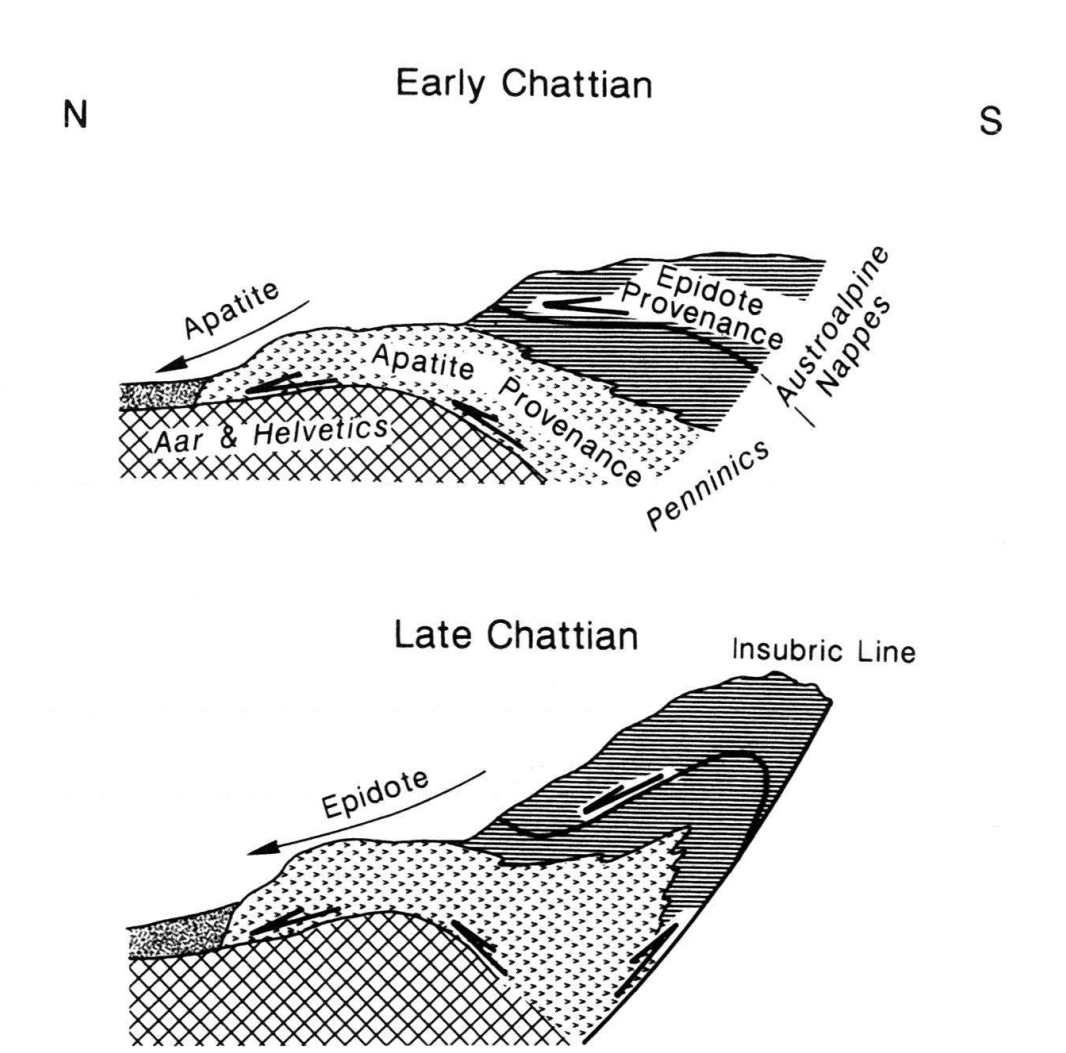


Fig. 12. Schematic diagram showing relationship of alpine evolution and source terrains during Early and Late Chattian times (for discussion see text).

nappes consisting mainly of carbonate and flysch units shed carbonate and sandstone clasts as well as abundant reworked apatite and zircon into the foreland basin (Fig. 12).

Fission track data indicate a rapid rate of uplift of the Sesia-Lanzo zone at 25 Ma. and of the Central Lepontine Alps at 24 Ma. (Hurford 1986, Hurford et al. 1991). This event was correlated by Schmid et al. (1987, 1989) with the Insubric phase of backthrusting which resulted in 15-20 km vertical displacement. Uplift increased the elevation of the higher Penninic and Austroalpine nappes. As a consequence of the higher relief, the drainage system cut farther and farther into the interior part of the Alps and the denudation rate of the structurally higher nappes increased drastically giving rise to the rapidly accumulating and prograding Blueme fan (Fig. 12). The erosional unconformity at its base also appears to be linked with this major tectonic event.

Progradation of the fan systems was accompanied by changing architectural styles, from meandering over sinuous to braided as well as a coarsening upward clast size. As a result of the outbuilding of the Blueme fan, local fans draining mainly marly and sandy flysch terrains were finally able to encroach laterally onto the fan. Moreover, the top beds of the Blueme fan are much younger in the Plateau Molasse (Langhian) than in the proximal (subalpine) area (Early Aquitanian). This could be explained by erosion, tectonic off-scaping or by burial by Alpine nappes, which because of the well-preserved geometry of the Blueme fan is the preferred interpretation. In essence, it appears that sedimentation ceased as the frontal Alpine nappes buried the proximal portion of the fan. Thus fan progradation and propagation of the alpine sole thrust towards the foreland occurred simultaneously.

8. Conclusions

- 1. The biostratigraphically well dated Subalpine USM of the Thun area and the autochthonous Molasse beneath span the time interval from Early Chattian to Early Aquitanian (~ 29 to 24 Ma) during which on average 4000 m of alluvial sediments were deposited corresponding to a mean sediment accumulation rate of 0.8 mmy⁻¹ (compaction ignored). However, the accumulation rate varies considerably both through time and spatially. For example, in the Blueme fan 1300 m were laid down during 0.5 Ma in the Prässerebach section whereas about 4000 m were deposited in the Thun section in 1 Ma, indicating accumulation rates of 2.6 mmy⁻¹ and 4 mmy⁻¹, respectively. These high values contrast markedly with the 0.2 mmy⁻¹ sediment accumulation rate of the proximal Upper Marine Molasse of the Entlebuch area (Keller 1990).
- 2. Based on litho- and petrofacies the stratigraphy of the USM is divided into six informal units which can be attributed to individual alluvial fans. The Early Chattian Schwändibach Conglomerate represents a 400 m thick small fan whereas the Homberg Beds and the Losenegg Beds constitute the much larger Honegg fan measuring almost 1000 m in thickness. The Late Chattian Thun Conglomerate constitutes the Blueme fan which with over 4000 m thickness in the proximal reaches is by far the largest fan in the study area. The Honegg Marls and the Gitzischöpf Conglomerate represent two local fans which encroached onto the Blueme fan.
- 3. Whereas the USM is well exposed in the Subalpine thrust belt, it is hidden by younger Molasse groups over most of the central and eastern segment of the Swiss Plateau. Previous reconstructions of the depositional history of the USM in this part of

the basin are based mainly on heavy mineral correlations of Subalpine Molasse and well sections of a few deep boreholes penetrating the Plateau Molasse (e.g. Schlanke 1974, Maurer et al. 1978). The combination of bio- and lithostratigraphic data and petrofacies from outcrops and deep boreholes with seismic data allows for the first time a controlled correlation of lithostatigraphic units of Subalpine and Plateau USM and reconstruction of the depositional history. This reveals that the Granitic Molasse in this part of the Plateau is the distal facies of the Honegg and Blueme fans and that the Late Chattian Gunten Quartzite Conglomerate correlates with the Burdigalian to Langhian conglomerates of the Plateau Molasse.

- 4. Sedimentation of the proximal Lower Freshwater Molasse at the southern margin of the foreland basin is closely linked with the rapid uplift of the Sesia-Lanzo Zone along the Insubric Line at ~ 25 Ma.
- 5. This uplift increased the elevation of the structurally higher upper Penninic and Austroalpine nappes. As a consequence the alpine drainage divide shifted southwards and the watershed of the river feeding the Thun Molasse increased.
- 6. The higher topographic gradient caused rapid erosion of these higher nappes and their crystalline cores producing an inverse sequence of unroofing recorded by the abrupt change in the composition of the detritus from mixed sedimentary/igneous to dominantly igneous. It also caused rapid progradation of the Blueme fan.
- 7. This rapid progradation resulted in strongly diachehronous facies relationships within the the alluvial fans and in a coarsening upward sequence.

Acknowledgments

The authors wish to thank B. Engesser, Cl. Mödden and M. Hugueney for identification of the micromammals, P. Allenbach for advice concerning the interpretation of the seismics and A. O. Pfiffner and M. Handy for stimulating discussions. H. Haas is thanked for her willingness and patience to carry out the countless heavy mineral separations and V. Grečo for preparation of thin sections. We also thank H. Haus for making available his unpublished map of the Thun Molasse. Special thanks go to BEB in Hannover, Germany for giving permission to publish the line drawing of a seismic section and the heavy mineral data of the Thun-1 borehole. The help of S. Burns and S. Hillier with the English is kindly acknowledged. The paper benefitted from the many helpful comments provided by the reviewers B. Keller and W. Wildi. Finally, F. S. thanks his collegues who acted as assistants, climbing instructors and baggage carriers. Partial support for this research was provided by the Swiss National Science Foundation (grant no. 21-36219.92).

REFERENCES

- BECK, P. 1911: Über den Bau der Berner Kalkalpen und die Entstehung der subalpinen Nagelfluh. Eclogae geol. Helv. 11, 497-518.
- 1923: Das stampische Alter der Thuner Nagelfluh und deren Bedeutung für den Bau des Alpenrandes. Mitt. natf. Ges. Bern XX.
- 1946: Über den Mechanismus der subalpinen Molassetektonik. Eclogae geol. Helv. 38, 353-368.
- BECK, P. & RUTSCH, R. F. 1958: Erläuterungen: Geologischer Atlas der Schweiz 1:25000, Bl. Münsingen-Konolfingen-Gerzensee-Heimberg (Nr. 21). Schweiz. geol. Komm.
- Berli, S. 1985: Die Geologie des Sommersberges (Kantone St. Gallen und Appenzell). Ber. St. gall. natf. Ges. 82, 112-145.
- BOLLIGER, T., GATTI, H. & HANTKE, R. 1988: Zur Geologie und Paläontologie des Zürcher Oberlandes. Vjschr. natf. Ges. Zürich 133, 1-24.
- Bown, T. M. & Kraus, M. J. 1987: Integration of channel and floodplain suites, I. Developmental sequence and lateral relations of alluvial paleosols. J. sediment. Petrol. 57, 587-601.

- BURBANK, D. W., ENGESSER, B., MATTER, A. & WEIDMANN, M. 1992: Magnetostratigraphic chronology, mammalian faunas, and stratigraphic evolution of the Lower Freshwater Molasse, Haute-Savoie, France. Eclogae geol. Helv. 85, 399-431.
- BURKHARD, M. 1988: L'Hélvetique de la bordure occidentale du massif de l'Aar (évolution tectonique et métamorphique). Eclogae geol. Helv. 81, 63-114.
- 1990: Aspects of the large-scale Miocene deformation in the most external part of the Swiss Alps (Subalpine Molasse to Jura fold belt). Eclogae geol. Helv. 83, 559-583.
- BUTLER, R. W. H. 1989: The geometry of crustal shortening in the western Alps. In: Tectonic Evolution of the Tethyan Region (Ed. by SENGÖR A. M.), Proc. NATO Advanced Study Institute, C239, 43-76.
- CANDE, S. C. & KENT, D. V. 1992: A new geomagnetic polarity timescale for the late Cretaceous and Cenozoic. J. Geophys. Res. 97, 13917-13951.
- DECELLES, P. G., GRAY, M. B., RIDGWAY, K. D., COLE, R. B., PIVNIK, D. A., PEQUERA, N. & SRIVASTAVA, P. 1991: Controls on synorogenic alluvial-fan architecture, Beartooth Conglomerate (Palaeocene), Wyoming and Montana. Sedimentology 38, 567-590.
- DIEM, B. 1986: Die Untere Meeresmolase zwischen der Saane (Westschweiz) und der Ammer (Oberbayern). Eclogae geol. Helv. 79, 493-559.
- ENGESSER, B. 1990: Die Eomyidae (Rodentia, Mammalia) der Molasse der Schweiz und Savoyens. Systematik und Biostratigraphie. Schweiz. paläont. Abh. 112, 1-144.
- ENGESSER, B. & MAYO, N. A. 1987: A biozonation of the Lower Freshwater Molasse (Oligocene and Agenian) of Switzerland and Savoy on the basis of fossil mammals. Münchner Geowiss. Abh. (A) 10, 67-84.
- FÜCHTBAUER, H. 1964: Sedimentpetrographische Untersuchungen in der älteren Molasse nördlich der Alpen. Eclogae geol. Helv. 57, 157-298.
- GASSER, U. 1968: Die innere Zone der subalpinen Molasse des Entlebuchs (Kt. Luzern), Geologie und Sedimentologie. Eclogae geol. Helv 61, 229-313.
- GIGER, M. 1991: Geochronologische und petrographische Studien an Geröllen und Sedimenten der Gonfolite Lombarda Gruppe (Südschweiz und Norditalien) und ihr Vergleich mit dem alpinen Hinterland. Unpubl. Ph.D. thesis, Univ. Bern.
- HABICHT, J. K. A. 1987: Schweizerisches Mittelland (Molasse). Internationales Stratigraphisches Lexikon EUROPA-EUROPE I/Fasc. 7b. Schweiz. Geol. Komm.
- HAUS, H. 1937: Geologie der Gegend von Schangnau im oberen Emmental (Kt. Bern). Ein Beitrag zur Stratigraphie und Tektonik der subalpinen Molasse und des Alpenrandes. Beitr. geol. Karte Schweiz (N. F.) 75. Schweiz. geol. Komm.
- HEWARD, A. P. 1978: Alluvial fan and lacustrine sediments from the Stephanian A and B (La Magdalena, Ciñera-Matallana and Sabero) coalfields, northern Spain. Sedimentology 25, 451-488.
- HOMEWOOD, P., ALLEN, P. A. & WILLIAMS, G. D. 1986: Dynamics of the Molasse Basin of western Switzerland. In: Foreland Basins. (Ed. by Allen, P. A. & Homewood, P.). Spec. Publ. int. Assoc. Sedimentol. 8, 199-217.
- HURFORD, A. J. 1986: Cooling and uplift patterns in the Lepontine Alps South Central Switzerland and an age of vertical movement on the Insubric fault line. Contrib. Mineral. Petrol. 93, 413-427.
- HURFORD, A. J., HUNZIKER, J. C. & STÖCKERT, B. 1991: Constraints on the late thermotectonic evolution of the Western Alps: Evidence for episodic rapid uplift. Tectonics 10, 758-769.
- HURNI, A. 1992: Geologie und Hydrogeologie des Truebtales. Unpubl. Diploma thesis, Univ. Bern.
- KAELIN, B., RYBACH, L. & KEMPTER, E. H. K. 1992: Rates of deposition, uplift and erosion in the Swiss Molasse Basin estimated from sonic- and density logs. Bull. Ver. schweiz. Petroleum-Geol. u.-Ing. 58, 9-22.
- Keller, B. 1990: Wirkung von Wellen und Gezeiten bei der Ablagerung der Oberen Meeresmolasse; Löwendenkmal und Gletschergarten zwei anschauliche geologische Studienobjekte. Mitt. natf. Ges. Luzern 31, 245–271.
- MANGE, M. A. & MAURER, H. F. W. 1992: Heavy Minerals in Colour. Chapman & Hall, London.
- MATTER, A. 1964: Sedimentologische Untersuchungen im östlichen Napfgebiet. Eclogae geol. Helv. 57, 315-428.
- MATTER, A., HOMEWOOD, P., CARON, C., RIGASSI, D., VAN STUIJVENBERG, J., WEIDMANN, M. & WINKLER, W. 1980: Flysch and Molasse of western and central Switzerland. In: Geology of Switzerland, a guidebook (Part B: Excursions), 261–293. Wepf, Basel.
- MAURER, H. 1983: Sedimentpetrographische Analysen an Molasseabfolgen der Westschweiz. Jb. geol. Bundesanst. (Wien) 126, 23-69.
- MAURER, H., FUNK, H. P. & NABHOLZ, W. 1978: Sedimentpetrographische Untersuchungen an Molasse-Abfolgen der Bohrung Linden 1 und ihrer Umgebung (Kt. Bern). Eclogae geol. Helv. 71, 497-515.

MAURER, H., GERBER, M. E. & NABHOLZ, W. K. 1982: Sedimentpetrographie und Lithostratigraphie der Molasse im Einzugsgebiet der Langete (Aarwangen-Napf, Oberaargau). Eclogae geol. Helv. 75, 381-413.

- MCBRIDE, E. F. 1963: A classification of common sandstones. J. sediment. Petrol. 33, 664-669.
- MIALL, A. D. 1978: Tectonic setting and syndepositional deformation of molasse and other nonmarine-paralic sedimentary basins. Canad. J. Earth Sci. 15, 1613.
- MIALL, A. D. 1985: Architectural element analysis: A new method of facies analysis applied to fluvial deposits. Earth-Sci. Rev. 22, 261-308.
- MICHOLET, J. 1992: Le puits de Thoune Forage d'exploration pétrolière en Suisse. Consortium Pétrolier Fribourgeois et Bernois. Bull. Ver. schweiz. Petroleum-Geol. u. -Ing. 58, 23-32.
- PIERSON, T. C. 1980: Erosion and deposition by debris flows at Mount Thomas, North Canterbury, New Zealand. Earth Surface Processes 5, 227-247.
- PLATT, N. H. & KELLER, B. 1992: Distal alluvial deposits in a foreland basin setting the Lower Freshwater Molasse (Lower Miocene), Switzerland: sedimentology, architecture and palaeosols. Sedimentology 39, 545-565.
- RENZ, H. H. 1937: Die subalpine Molasse zwischen Aare and Rhein. Eclogae geol. Helv. 30, 87-214.
- Rust, B. R. 1978: Depositional models for braided alluvium. In: Fluvial Sedimentology (Ed. by MIALL, A. D.). Mem. Can. Soc. Petrol. Geol. 5, 221-245.
- Scherer, F. 1966: Geologisch-palaeontologische Untersuchungen im Flysch und in der Molasse zwischen Thunersee und Eriz (Kt. Bern). Beitr. geol. Karte Schweiz (N. F.) 127. Schweiz. geol. Komm.
- SCHLANKE, S. 1974: Geologie der Subalpinen Molasse zwischen Biberbrugg SZ, Hütten ZH und Ägerisee ZG, Schweiz. Eclogae geol. Helv. 67, 243-331.
- SCHLUNEGGER, F. 1991: Stratigraphie, Sedimentologie und Tektonik der Unteren Süsswassermolasse östlich von Thun. Unpubl. Diploma thesis, Univ. Bern.
- 1994: Magnetostratigraphie und fazielle Entwicklung der Unteren Süsswassermolasse zwischen Aare und Limmat. Ph. D. thesis Univ. Bern.
- SCHMID, S. M., ZINGG, A. & HANDY, M. 1987: The kinematics and movement along the Insubric line and the emplacement of the Ivrea Zone. Tectonophysics 135, 47-66.
- SCHMID, S. M., AEBLI, H. R., HELLER, F. & ZINGG, A. 1989: The role of the Periadriatic Line in the tectonic evolution of the Alps. In: Alpine Tectonics (Ed. by COWARD, M., DIETRICH, D. & PARK, R. G.). Geol. Soc. Spec. Publ. 45, 153-171.
- SINCLAIR, H. D., COAKLEY, B. J., ALLEN, P. A. & WATTS, A. B. 1991: Simulation of foreland basin stratigraphy using a diffusion model of mountain belt uplift and erosion: an example from the central Alps, Switzerland. Tectonics 10, 599-620.
- SMITH, N. D. 1974: Sedimentology and bar formation in the Upper Kicking Horse River, a braided outwash stream. J. Geol. 82, 205-224.
- SPECK, J. 1953: Geröllstudien in der subalpinen Molasse am Zugersee und Versuch einer paläogeographischen Auswertung. Ph. D. thesis, Univ. Zürich.
- STÄUBLE, M. & PFIFFNER, O. A. 1991: Processing interpretation and modeling of seismic reflection data in the Molasse Basin of eastern Switzerland. Eclogae geol. Helv. 84, 151-175.
- STEEL, R. J., MAEHLE, H. R., RØE, S. L. & SPINNANGR, Å. 1977: Coarsening-upward cycles in the alluvium of Hornelen Basin (Devonian), Norway. Bull. geol. Soc. Am. 88, 1124-1134.
- STUDER, B. 1825: Beyträge zu einer Monographie der Molasse. Jenni, Bern.
- TRÜMPY, R. 1960: Paleotectonic evolution of the Central and Western Alps. Bull. geol. Soc. Amer. 71, 843-908.
- TRÜMPY, R. & BERSIER, A. 1954: Les éléments des conglomérats oligocènes du Mont-Pélerin. Eclogae geol. Helv. 47, 119-166.
- VOLLMAYR, T. 1992: Strukturelle Ergebnisse der Kohlenwasserstoffexploration im Gebiet von Thun, Schweiz, Eclogae geol. Helv. 85, 531-539.
- ZIMMERMANN, M. A., KÜBLER, B., OERTLI, H. J., FRAUTSCHI, J.-M., MONNIER, F., DERES, F. & MONBARON, M. 1976: Molasse d'eau douce inférieure du plateau Suisse. Subdivision par l'indice détritisme; essai de datation par nannofossiles. Bull. Centre Rech. Pau SNPA 10, 585–625.

Manuscript received 15 March 1993 Revision accepted 13 August 1993

| | Section | | | | | ι | 10 | 11 | ၁ | s | ι | ıo | BG | qe | 16 | S | SE | :1, | Ы | | | | | | | u | oi: | to | Э | s | uı | ոպ | 1 | | |
|---------------|----------------------|--------|--------|--------|--------|--------|--------|--------|--------|--------|----------|----------------|--------|--------|--------|---------|--------|--------|----------|-------------|----------|--------|---------|---|--------|-----------|--------|----------|--------|--------|--------|------------------|--------|--------|------------|
| | ţinU | | | | | 0 | 7 | | | | | ü | Н | | | n | e | | 200 | = 5 E | | !9 | | | | ч | ၁ | s | | | | o S F O | ū | Н | |
| | Number of clasts (N) | 172 | 211 | 178 | 165 | 170 | 171 | 164 | 172 | 380 | 188 | 162 | 177 | 152 | 152 | 187 | 167 | 134 | 161 | 278 | 162 | 165 | 165 | 214 | 199 | 206 | 174 | 245 | 209 | 192 | 210 | 220 | 172 | 232 | 221 |
| | ### Partzite | 0 | 0 | 5.6 | | | | 0 | 0 | 0 | 0 | 0 | ~ | 0 | | 12 | Ξ | 26.9 | 0 | 0 | | 0 | | 0 | | | | | 0 | | | 0 | 0 | 0 | ٠ <u>۱</u> |
| | Total sedimentary | 61.6 | 52.9 | 55. | .99 | 52.9 | 48.7 | 58.1 | 61.5 | 66 | 25 | 30.5 | 44.1 | 35.5 | 29.6 | 54.5 | 30.4 | 29 | 06 | 100 | 54.8 | 91.8 | 59.7 | 58.9 | 72 | 63.5 | 8.69 | 71.2 | 70.3 | 59.2 | 51.4 | 54.2 | | | 49.5 |
| | Sandstone | 18.6 | 3.8 | 7.3 | -1 | 5.3 | 1.1 | 9.1 | 18.6 | 0 | 4.3 | 7 | 11.3 | 5.9 | 4.6 | 29.4 | 12.6 | 11.9 | 38.4 | 93.2 | 7.3 | 21.6 | | 4.7 | | | 8.6 | | 2.4 | 5.7 | 8.6 | | | 10.3 | |
| | Dolomite | 5.2 | 1.9 | 2.2 | 4.2 | 1.7 | 6.4 | 9.1 | 5.5 | 20 | 0 | 1.9 | 1.7 | 0 | 0 | 0 | 0 | 0 | 0 | 0 | 0 | 0 | 0 | 4. | 4 | - | 1.7 | 5.3 | 3.3 | 2.1 | 2.9 | 1.8 | 5.2 | 4.3 | 4.4 |
| | Chert | 2.3 | 3.3 | 4.5 | N | 6.5 | 1.8 | 2.4 | 2.2 | | 0 | 1.9 | 0 | 1.3 | 1.3 | 0 | _ | 0 | 1.3 | 0 | 0 | 4.2 | 9 | 4.2 | 2.5 | 2.9 | 8 | 1.6 | 4.3 | 4.2 | 4. | 2.7 | 1.7 | _ | F |
| S | lstoT | 35.5 | 43.9 | 41.2 | 49.7 | 39.4 | 29.4 | 37.5 | 35.5 | 79 | 20.7 | 19.7 | 31.1 | 28.3 | 23.7 | 25.1 | 16.8 | 17.1 | 50.3 | 5.8 | 47.5 | 99 | 50.7 | 48.6 | 57.5 | 47 | 56.3 | 8.69 | 60.3 | 47.2 | 38.5 | 38.8 | 38.5 | 38.4 | 38.9 |
| Limestones | Siliceous | 25.6 | 34.9 | က | 4 | | | 28.4 | | | 14.8 | 15.4 | 22.6 | 14.5 | 6.6 | 9.6 | 12 | 5.5 | 39.5 | | 34.5 | 37 | 39.5 | 42.2 | 20 | 40.5 | 44.8 | 52.9 | 49.8 | 38.9 | 26.6 | 30.2 | 24.5 | 29.8 | 28 |
| 5 | Non-siliceous | 6.6 | o | 11.2 | 9.7 | 5.3 | 5.8 | 9.1 | 6.6 | | 6.3 | 4.3 | 8.5 | 13.8 | 13.8 | 15.5 | 4.8 | 11.9 | 10.8 | | 13 | | 11.5 | 6.1 | 7.5 | 8.9 | 11.5 | 6.9 | 10.5 | 8.3 | 11.9 | 8.6 | 4 | 8.6 | 10.9 |
| | Total crystalline | 38.4 | 47.1 | 42.2 | 33.1 | 47.1 | 51.3 | 41.9 | 38.5 | 7 | 75 | 69.5 | 55.3 | 64.5 | 54 | 33.4 | 58.5 | 44.1 | 10 | Ţ | | 8.2 | 40.3 | 41.1 | 28 | 36.5 | 30.2 | 28.8 | 29.7 | 40.8 | 48.6 | 45.8 | 52.3 | 47 | 50.5 |
| | Metamorphic | = | 9.5 | 13.5 | 5.4 | 4.6 | 6.6 | 14.6 | Ξ | | 14.3 | 18.5 | 17.5 | 7.9 | 6.6 | 2.7 | 18 | 4.5 | N | 0 | 9.8 | 1.2 | 6.4 | 0 | 5.5 | 8.9 | 80 | 4.1 | 9.1 | 11.5 | 14.8 | 14.5 | 23.3 | 15.5 | 18.6 |
| | Volcanics | 4.7 | 10.9 | 7.9 | 12.7 | 16.7 | 21.1 | 8.5 | | | 7.4 | - - | თ | 5.3 | 14.4 | -: | o | 3.8 | ⊽ | 0 | 10.5 | | 13.5 | ر. ک | 4 | 11.7 | 10.3 | 10.2 | 4.8 | 7.8 | 5.7 | 7.7 | 1.2 | 2.5 | 6 |
| | Vein quartz | 4.1 | 2.4 | 4.5 | 3.6 | 5.3 | 4.1 | 0 | 4.1 | | 10.1 | 6.8 | 11.3 | 7.2 | 7.9 | 6.4 | | 10.4 | ιο · | ٥ | 3.7 | 0 | - | 4. | - ! | <u>ი</u> | 2.3 | 1.6 | 6.2 | 1.7 | 6.2 | | | 4.7 | |
| | Muscovite granite | 10.5 | 13 | 5.1 | 4.2 | 4.1 | 8.6 | 5.5 | 10.5 | | 10.6 | 7 | 0 | 4.6 | 3.3 | 2.9 | 10.2 | 8.2 | - | 9 | 1.2 | | 2.5 | 4. | 4 (| 8.0 | 1.7 | 3.8 | 0 | 8.9 | 6.2 | | 1.7 | , | - |
| ites | Leucocratic granite | 0 | 9.9 | 6.2 | 3.6 | 7.1 | 2.3 | 1.8 | 0 | | 4.8 | | 4 | ٥ | 5.6 | 2.7 | 9.9 | 9 | <u>,</u> | • | <u>~</u> | 4 | 2.5 | 2.0 | 0.0 | N . | 4.6 | 4.5 | 5.3 | 3.1 | 4. | 3.2 | 1.7 | - , | - - |
| Granites | Ped granite | 3.5 | 1.9 | - | 3.6 | 3.5 | 1.8 | 3.6 | 3.5 | 1 | 20.7 | 20.4 | 12.4 | 31.6 | 15.9 | 6.9 | 9 | 8.2 | 0 | 0 | | 0 | - · | 4 (| 0.0 | 4 (D) | 2.3 | 3.6 | - | 3.1 | 12.9 | 7.7 | | | 0 |
| | Green granite | 4.6 | 2.8 | 3.9 | 0 | - | 2.3 | 3.7 | 4.7 | 1 | 6.4 | 4.9 | | 7.9 | 0 | 6.4 | 4.8 | 6 | Ţ | 0 | 6.4 | | ?; 8 | , , | | Ç. | - | ⊽ | 3.3 | 4.7 | 4. | 3.2 | 3.5 | | |
| | Gabbro | 0 | 0 | 0 | 0 | 0 | 1.2 | 4.2 | 0 | | <u>~</u> | 0 | 0 | 0 | 0 | 4 6. | 1.2 | 0 | _ | 0 | 3.7 | 0 | _ | _ | 5 0 | 0 | 0 | <u> </u> | 0 | 0 | 0 | Į. | 3.5 | 2.6 | Ž |
| | Elevation | 730 | 730 | 740 | 750 | 750 | 760 | 760 | 765 | 780 | | 820 | 840 | 870 | 910 | 1060 | 1080 | 1100 | 1063 | 10/0 | 1070 | | | 9 0 | 0 0 | 050 | 630 | | 780 | 069 | 730 | | 790 | 640 | 1089 |
| grid | 926 | 181500 | 181500 | 181425 | 181400 | 181250 | 181175 | 181150 | 181100 | 181075 | 180950 | 180725 | 180300 | 180050 | 179625 | 179325 | 179175 | 1/8600 | 178600 | 1/8500 | 178450 | 178350 | 1/8300 | 0000 | 100700 | 001081 | 180075 | 179750 | 179425 | 179725 | 179550 | 179425 | 179425 | 178900 | 1,65/5 |
| National grid | reference | 621550 | 621600 | 621700 | 621925 | 622025 | 622150 | 622225 | 622425 | 622325 | 622300 | 622275 | 622350 | | | 623650 | 624050 | 623/00 | | | _ | 624000 | 646995 | 0 | 0000 | 000000 | 615800 | 616425 | 616325 | 615900 | 615900 | 614850 | 615900 | 615250 | 1004010 |

Table 1. Conglomerate clast count data of different units of the Subalpine Molasse. For unit abbreviations see Table 2.

| | tinU | οн | ΡΟ | üН | пŋ | ион | G! |
|---------------|----------------------|--|--|--|---|--------------------------------------|---|
| | Anatase & Brookite | 04000 | -000 | 0000-00-00 | 0 0 0 | 3 5 5 | 0000- |
| | Garnet | 185 281 167 100 206 564 | 123 416 520 028 690 498 | 103 174 174 80 64 66 60 17 72 | 1 0 4 4 4 4 4 4 4 4 4 4 4 4 4 4 4 4 4 4 | 33 104 146 182 | 462 66 152 143 293 |
| | lstoT | 000000 | 000000 | 000000000000000000000000000000000000000 | 100 | 100 | 10000 |
| | Others | 0000-0 | 0000-0 | 00000000 | -0- | 8 - 8 7 | 0 6 - 0 0 |
| | Serpentine | 000000 | 000000 | 00001-0000 | 000 | 0000 | 00000 |
| T | Pumpellyite | 000000 | 000000 | 000004-4 | 0 8 0 | 0000 | 00000 |
| | Lawsonite | 000000 | 000000 | 000000000 | 000 | 0000 | 00000 |
| | Blue sodic amphibole | 000000 | 000000 | 000000-00 | 000 | 0000 | 00000 |
| | Chromian spinel | - 60000 | 00000 | 00-000000 | 000 | 00 | 0000- |
| Group | IstoT | 000000 | 000000 | 0000040817 | 000 | 0000 | 00000 |
| e Gr | Diallage | 00000 | 000000 | 00000000000 | 000 | 0000 | 00000 |
| Pyroxene | Нурегатьепе | 00000 | | | | | 00000 |
| Py | Augite & Diopside | 00000 | 00000 | 0000040000 | 000 | | |
| | Tremolite | 00000 | | | | | 00000 |
| | lstot | 00000 | | 000000074- | | | 00000 |
| nde | other types | 000000 | 000000 | 000000000 | 000 | 0000 | 00000 |
| Hornblende | prown | 000000 | 000000 | 00000000 | 000 | 0000 | 00000 |
| 운 | green-brown | 00000 | | 2 | | | 00000 |
| | blue-green | 00000 | | 000000004- | | | 00000 |
| | Sphene | 00000 | _ | ۵. | | | |
| | Staurolite | | 10 20 33 33 28 | | | | |
| | Rutile | 4 4 0 0 0 - | W 4 4 - 0 V | 0-0000-0-0 | | | 0 - 10 0 |
| | Tourmaline | 22 10 20 21 30 | 2 4 4 1 0 0 0 0 0 0 0 0 0 0 0 0 0 0 0 0 0 | 80 - 88 - 8 - 8 | - 6, 4 | 2 1 1 2 2 4 | 0 - 0 0 |
| | Zircon | 00000 | 8 9 8 4 9 4 | 200000000000000000000000000000000000000 | 0 4 0 | 1 2 6 | |
| | Apatite | 0 59 0 50 8 59 6 48 6 48 | 2 61 7 42 1 60 2 37 2 34 2 41 | 5 3 3 3 5 5 5 5 5 5 5 5 5 5 5 5 5 5 5 5 | | 3 45 5 30 6 34 3 15 | 5 51 6 8 7 28 6 1 6 1 3 50 |
| | Total | - | | 2 2 2 2 2 2 3 4 2 2 3 4 4 4 4 4 4 4 4 4 | 4 68 2 67 4 80 | 0000 | - 8 4 8 0 |
| ٩ | Composite grains | 000000 | 00000 | 00 22 00 38 00 42 00 21 00 21 00 27 00 27 | | 0000 | 0 0 0 0 0 4 4 0 0 0 0 0 0 0 0 0 0 0 0 0 |
| Group | Saussurite | 00-000 | 0 0 0 - 0 0 | 200-0-1-000 | 00- | 0000 | 00000 |
| Epidote | ətinsllA | 00000 | 000000 | 000000000000000000000000000000000000000 | 8 2 2 | 0000 | 0 - 0 - 0 |
| Ē | efisioZ | 004000 | -00-00 | | 100 Miles | 6 4 1 | |
| | Clinozoiste | 00000- | 200-00 | 460 | 6 30 0 33 0 43 | 0000 | 8 |
| - | etobiq∃ | | 3000 100 3000 2000 1000 | 323 -3 | 0 16 0 20 0 30 | | 2 2 + + |
| | Elevation | 710 750 790 690 700 700 | 760 760 760 770 770 780 | 790 810 830 850 870 850 870 870 | 910 920 950 | 1056 960 1070 1070 | 1080 1120 1130 1130 |
| Þ. | | 182175 182080 182200 181900 181950 | 181425 181425 181175 181150 181075 | 180950 180750 180725 180575 180475 180350 180150 180050 | 179650 179425 178750 | 179175 178675 178350 178375 | 178500 178400 178350 178300 |
| al gr | reference | | | | | | |
| National grid | refer | 620450 620725 621080 620650 620925 621450 | 621775 621900 622150 622225 622350 622350 | 622300 622350 622100 622450 622450 622625 622625 622750 | 623100 623350 623750 | 624150 623750 623925 623925 | 623925 624000 624000 624000 |
| Z | | 000000 | 9 9 9 9 9 | 0000000000 | 9 9 | 9 9 9 | 9 9 9 9 |

Table 2. Heavy mineral data of different lithostratigraphic units in the Prässerebach section. Sch = Schwändibach Cgl., Ho = Homberg Beds, Lo = Losenegg Beds, Hü = Hünibach Cgl., Gu = Gunten Quartzite Cgl., Hon = Honegg Marls, Gi = Gitzischöpf Cgl.

ūН gcp S LO JinU 00000000000000000 Anatase & Brookite 23 247 100 909 100 97 100 258 100 580 53 816 100 687 816 Garnet Total Others Serpentine 0000000 Pumpellyite 000000 0000000 0000 Lawsonite 000000 000000 Blue sodic amphibole 000000 Chromian spinel Pyroxene Group Total Diallage 0000000 0000 Hypersthene ebisqoid & etiguA 000000 0000 000000 I remolite total Hornblende other types prown green-brown pine-green Sphene Staurolite **elituR** Tourmaline **Zircon** etitsqA Total Composite grains **Epidote Group** 0000 000-00 Saussurite -000 -0000 0000-00 **etinsllA** efisioZ 00000 12 20 27 12 12 31 Clinozoiste 100 etobiq3 Elevation 616000 180175 615825 179950 615900 179700 615900 179675 616250 179275 615250 178925 615825 179975 616450 179750 615900 179650 614875 179375 614875 179325 615875 179475 616425 179450 National grid reference

Fable 2 (continued)

| | Anatase & Brookite | c | , 0 | 0 | 0 | 8 | 0 | 0 | 0 | 0 | 0 | 0 | 0 | 0 | 0 | 0 | - | - | 0 | - | 0 | - | 0 0 | o c | ۰ ۸ | 4 | _ | - | 0 | 0 | 0 | - | 7 | 0 | 0 |
|---------------|----------------------|-----|------|------|-----|-----|-----|-----|-----|-----|-----|-----|-----|-----|------|-----|------|------|------|------|------|----------|------|------------|------|------|------|------|------|------|------|------|------|------|------|
| | Garnet | 20 | 17 | . o | 9 | 8 | 15 | 8 | 4 | 20 | 8 | 18 | 19 | 6 | 34 | 4 | 38 | 25 | 4 4 | 64 | 122 | 80 | 31 | 7 0 | 51 | 130 | 258 | 160 | 48 | 63 | 128 | 93 | 147 | 546 | 98 |
| | Total | - | | | _ | _ | _ | _ | _ | _ | _ | | _ | _ | _ | _ | _ | _ | _ | _ | _ | _ | _ | | _ | _ | _ | | | | | 100 | 00 | 001 | 00 |
| | Others | + | - 50 | - 10 | | - | _ | _ | - | 16 | | | 100 | | 700m | | | | | | | | | | | _ | | Desc | 1000 | 9/00 | | 0 | 0 | 0 | 0 |
| | Serpentine | 6 | , c | | 0 | 0 | 0 | 0 | 0 | 0 | 0 | 7 | က | s. | 4 | - | - | - | - | 0 | 0 | 0 | 0 0 | - | . 0 | 0 | 0 | 7 | 0 | 0 | 0 | 0 | 0 | 0 | 0 |
| | Pumpellyite | 6 | , 0 | | | 8 | 0 | 7 | - | - | - | က | - | - | 0 | - | 0 | - | 0 | 0 | 0 | 0 | 0 (| . | | 0 | 0 | 0 | 0 | 0 | 0 | 0 | 0 | 0 | 0 |
| | Lawsonite | 6 | , 0 | | 0 | 0 | 0 | 0 | 0 | 0 | 0 | 7 | 0 | 0 | 0 | 0 | 0 | - | 0 | 0 | 0 | 0 | 0 0 | - c | | 0 | 0 | - | 0 | 0 | 0 | 0 | 0 | 0 | 0 |
| | Blue sodic amphibole | 6 | , 0 | ٠ 4 | 4 | 0 | 0 | 0 | N | 0 | 0 | - | - | - | 0 | 0 | 0 | 2 | 0 | 0 | 0 | 0 | 0 (| o c | . 0 | - | 0 | 0 | 0 | 0 | 0 | 0 | 0 | 0 | 0 |
| | Chromian spinel | - | . 0 | | 0 | 2 | 0 | - | - | - | 0 | 0 | - | 4 | - | 0 | _ | 0 | က | - | 0 | 0 | - , | | . m | 0 | က | - | က | - | 4 | 8 | 4 | - | 3 |
| 9 | Total | - | - (* |) 0 | 0 | 4 | 2 | က | 2 | 19 | 23 | 12 | 16 | 32 | 0 | 0 | 0 | 0 | 0 | 0 | _ | 0 | 0 (| - c | . 0 | 0 | 0 | - | 0 | - | 0 | - | 0 | 0 | |
| e Group | Diallage | 6 | , 0 | , , | 0 | 0 | 0 | 0 | 0 | 0 | 0 | 0 | 0 | 0 | 0 | 0 | 0 | 0 | 0 | 0 | 0 | 0 | 0 (| - c | . 0 | 0 | 0 | 0 | 0 | 0 | 0 | 0 | 0 | 0 | |
| Pyroxene | Hypersthene | 6 | , ~ | 1 0 | . 0 | 8 | N | - | 0 | 4 | က | - | က | 4 | 0 | - | 0 | 0 | 0 | 0 | 0 | 0 | 0 (| - c | . 0 | 0 | 0 | - | 0 | 0 | 0 | 0 | 0 | 0 | 0 |
| 1 | Augite & Diopside | - | | . c | 0 | N | က | N | သ | 15 | 20 | Ξ | 13 | 28 | 0 | თ | 0 | 0 | 0 | 0 | - | 0 | 0 (| - | , 0 | 0 | 0 | 0 | 0 | - | 0 | - | 0 | 0 | |
| Г | -Tremolite | 6 | , - | | , – | က | - | က | 0 | 0 | 0 | 0 | 0 | 0 | 0 | 0 | 0 | 0 | 0 | 0 | 0 | 0 | 0 (| - | , 0 | 0 | 0 | 0 | 0 | 0 | 0 | 8 | 0 | 0 | |
| П | lstot | 32 | 1 6 | 44 | 52 | 43 | 32 | 27 | 45 | 34 | 39 | 22 | 37 | 29 | ო | 63 | 0 | 5 | ო | 0 | ო | က | 9 (| n c | , ro | 0 | က | 7 | 7 | = | 8 | 10 | ი | 13 | 6 |
| ge | other types | 6 | > 4 | · · | · = | 4 | 4 | 10 | Ξ | 9 | က | - | 2 | 7 | - | က | 0 | 8 | 7 | 0 | - | 0 | - (| o c | 0 | 0 | 0 | 0 | 0 | 0 | 0 | 0 | 0 | - | 9 |
| Hornblende | prown | c | , , | ו ע | , n | 5 | 8 | 2 | 7 | 2 | 0 | - | 2 | 4 | 0 | = | 0 | 0 | 0 | 0 | 0 | 0 | ~ | - | | 0 | 0 | 0 | 0 | 0 | 0 | 7 | 0 | 0 | 7 |
| 본 | green-brown | - | - ~ | , , | 9 | 9 | 4 | က | S | 8 | 4 | 8 | 7 | 0 | 0 | 12 | 0 | 2 | 0 | 0 | 0 | 0 | 0 (| o c | 0 | 0 | - | 0 | 0 | 7 | က | 0 | 0 | 4 | 9 |
| | plue-green | 2 | 25 | 2 6 | 32 | 20 | 16 | 12 | 22 | 21 | 30 | 18 | 20 | 13 | 8 | 37 | 8 | 80 | - | 0 | 7 | - | e (| , (| 2 | 0 | 8 | 7 | 7 | 6 | 2 | 80 | 6 | 8 | 7 |
| | Sphene | - | | 0 | 1 0 | - | N | N | - | က | က | က | က | 0 | s, | - | 80 | N | Ξ | 9 | S | 4 | m . | 4 , | 0 | 0 | 0 | 0 | 0 | 0 | 0 | 0 | 0 | 0 | - |
| | Staurolite | - | - 0 | ۰ ، | 0 | - | 8 | 0 | - | 0 | - | - | 0 | - | 0 | 0 | 0 | - | 0 | က | - | ω . | α, | - 0 | 0 | - | - | 8 | 0 | 0 | 0 | 0 | က | 8 | 2 |
| | elituR | 6 | , c | | 0 | 0 | 0 | က | 0 | - | 0 | 0 | 0 | 0 | 0 | 0 | 0 | 0 | 0 | 0 | 0 | 0 | - (| v - | 4 | - | 8 | 8 | 7 | က | - | - | 7 | 0 | - |
| | Tourmaline | c | , - | | 0 | 8 | 0 | - | 0 | 0 | - | 0 | 8 | - | 8 | - | 0 | N | 7 | - | 4 | - | 4 (| v a | 4 | 9 | 6 | 16 | 13 | 13 | ဖ | Ξ | 18 | 13 | 4 |
| | Zircon | 0 | , - | ٠ ٣ | - | - | 2 | 2 | 0 | - | - | 0 | 8 | 7 | က | - | 8 | က | 9 | 4 | 16 | 4 | 9 | v c | , = | 13 | 13 | 17 | Ξ | Ξ | 13 | လ | 4 | 80 | 15 |
| | Apatite | ď | , 4 | | · e | 7 | က | 9 | 4 | 4 | 7 | 9 | 2 | 9 | 13 | 7 | 19 | 13 | 20 | 17 | 13 | 26 | 23 | 9 6 | 46 | 69 | 58 | 52 | 68 | 54 | 63 | 59 | 99 | 54 | 9 |
| | Total | 56 | 57 | 36 | 37 | 37 | 53 | 50 | 40 | 36 | 29 | 43 | 29 | 18 | 65 | 20 | 67 | 99 | 49 | 68 | 22 | 42 | 54 | 20 | | e | = | 4 | - | 9 | 2 | 6 | 4 | 6 | - |
| | Composite grains | 16 | | , v | . 5 | 8 | 4 | 4 | Ξ | 8 | 4 | 9 | 9 | - | က | 0 | 2 | 4 | 4 | 2 | 4 | 4 1 | , a | - 0 | . 0 | 0 | - | 0 | 0 | 0 | 0 | 0 | 0 | 0 | 9 |
| go | Saussurite | ~ | , « | , - | , | - | N | - | N | 0 | က | - | - | - | 0 | 0 | - | 8 | 0 | 0 | 0 | 0 | 0 (| - | 0 | 0 | 0 | 0 | 0 | 0 | 0 | 0 | 0 | 0 | 0 |
| ote G | Allanite | c | , 0 | | 0 | 0 | 0 | - | - | 2 | 0 | 0 | 0 | 0 | 0 | 0 | 0 | 0 | 0 | 0 | 0 | 0 | 0 (| o c | 0 | 0 | 0 | 0 | 0 | 0 | 0 | 0 | 0 | - | 0 |
| Epidote Group | Soisite | - | | ٠, | 0 0 | - | 0 | 4 | 4 | - | - | က | 8 | 0 | 2 | 0 | 7 | - | က | 8 | N | 0 | - (| າເ | 0 | 0 | 0 | 0 | 0 | 0 | 0 | 0 | 0 | 0 | 0 |
| | Olinozoiste | 00 | 0 | 9 00 | 13 | 28 | 29 | 27 | 8 | 18 | 15 | 21 | 14 | 12 | 19 | 20 | 33 | 56 | 21 | 33 | 20 | <u>.</u> | 6 | 22 | 2 | 0 | 7 | - | 0 | က | က | 4 | 7 | က | - |
| \prod | etobiq3 | 4 | . 6 | 2 0 | ^ | S | ۵ | 13 | 4 | 7 | 9 | 12 | 9 | 4 | 38 | 0 | 21 | 23 | 21 | 28 | 31 | 25 | 29 | - 6 | ^ | - | 80 | က | - | က | 8 | S | 8 | 2 | 0 |
| | Sample Depth (m) | 250 | 300 | 350 | 400 | 450 | 200 | 550 | 009 | 650 | 700 | 750 | 800 | 850 | 900 | 950 | 1000 | 1050 | 1100 | 1150 | 1200 | 1250 | 1300 | 330 | 1450 | 1500 | 1550 | 1600 | 1650 | 1700 | 1750 | 1800 | 1850 | 1900 | 1950 |

Table 3. Heavy mineral data of Molasse in the Thun-1 well.

| | Anatase & Brookite | 0000 | ٠- | υ 4 | 00 | · ~ | | - 0 | - 0 | 0 | - | 0 0 | 0 | 0 0 | · - | 0 | - (| 0 0 | > 0 | , 0 | , – | 8 | 0 0 | 2 |
|---------------|----------------------|----------------------|----------|----------------|-------------|------|------|------|------------|------|------|------|------|---------------|------|------|------|---------------|----------------|------|------|------|------|------|
| | Garnet | 81 280 121 | 301 | 285 | 227 | 87 | 91 | 37 | 4 a | 1 4 | 243 | 33 | 32 | 7 4 7 | 2 4 | 17 | 34 | 30 | 2 5 | 124 | 55 | 139 | 131 | 0 |
| | Total | 8 6 6 6 | 9 | 001 | 100 | 100 | 0 0 | 000 | 100 | 90 | 100 | 000 | 100 | 000 | 100 | 100 | 100 | 000 | 2 6 | 000 | 100 | 100 | 100 | 3 |
| | Others | 0-0- | - 0 | 00 | 00 | 0 | 0 0 | 0 | 0 0 | 0 | 0 | 0 0 | - | 0 0 | 0 | 0 | 0 0 | n c | > C | · - | . 0 | - | 0 1 | -1 |
| | Serpentine | 0 4 - 0 0 | 0 | 00 | 00 | 0 | 0 0 | 0 | 0 0 | 0 | 0 | 0 0 | 0 | 0 0 | 0 | 0 | 0 0 | o c | > 0 | , 0 | 0 | 0 | 0 0 | , |
| | Pumpellyite | 0000 | - | 00 | 00 | 0 | 0 0 | 0 | 0 0 | 0 | 0 | 0 0 | 0 | 0 0 | 0 | 0 | 0 0 | 5 C | > 0 | , 0 | . 0 | 0 | 0 0 | , |
| | Lawsonite | 0000 | 0 | 00 | 00 | 0 | 0 0 | 0 | 0 0 | 0 | 0 | 0 0 | 0 | 0 0 | 0 | 0 | 0 0 | 5 C | > 0 | , 0 | , 0 | 0 | 0 0 | > |
| | Blue sodic amphibole | 0000 | 0 | 0 0 | 00 | 0 | 0 0 | 0 | 00 | 0 | 0 | 0 0 | 0 | 0 0 | 0 | 0 | 0 (| 5 C |) C | , 0 | , 0 | 0 | 0 0 | > |
| | Chromian spinel | 10000 | 0 | 0 0 | e - | - | 0 0 | 0 | 0 - | . 0 | 0 | 0 0 | - | o + | - 0 | 0 | 0 0 | 5 C | > 0 | , 0 | , 0 | - | 0 0 | > |
| Group | IstoT | , r o o c | 1 (1 | - 0 | 00 | | 0 0 | 0 | 0 0 | 0 | 0 | 0 0 | 0 | 0 0 | 0 | 0 | 0 0 | 5 C | > 0 | , 0 | , 0 | 0 | 0 0 | > |
| e Gre | Diallage | 0000 | 0 | 00 | 00 | 0 | 0 0 | 0 | 0 0 | 0 | 0 | 0 0 | 0 | 0 0 | 0 | 0 | 0 (| 5 0 | > 0 | , 0 | . 0 | 0 | 0 0 | > |
| Pyroxene | Hypersthene | 0000 | 0 | 00 | 00 | 0 | 0 0 | 0 | 0 0 | 0 | 0 | 0 0 | 0 | 0 0 | 0 | 0 | 0 0 | 5 C | > C | , 0 | 0 | 0 | 0 0 | > |
| Ą | Augite & Diopside | 0000 | 7 72 | - 0 | 00 | | 0 0 | 0 | 0 0 | 0 | 0 | 0 0 | 0 | o c | 0 | 0 | 0 0 | 5 C | > 0 | , 0 | 0 | 0 | 0 | , |
| | Tremolite | 0000 | 0 | 00 | 00 | | 0 0 | 0 | 0 0 | 0 | 0 | 0 0 | 0 | o c | 0 | 0 | 0 0 | - | > 0 | , 0 | . 0 | 0 | 0 0 | > |
| | lstot | | 1 4 | 00 | 00 | 0 | 0 0 | 0 | 0 0 | 0 | 0 | 0 0 | 0 | 0 0 | 0 | 0 | 0 0 | 5 C | > C | , 0 | . ~ | 2 | 0 0 | > |
| nde | other types | ,-0 | - 0 | 00 | 00 | 0 | 0 0 | 0 | 0 0 | 0 | 0 | 0 0 | 0 | o c | 0 | 0 | 0 0 | 5 C | > < | , 0 | . 0 | 0 | 0 0 | > |
| Hornblende | prown | 0-0 | - 0 | 00 | 00 | 0 | 0 0 | 0 | 0 0 | 0 | 0 | 0 0 | 0 | o c | 0 | 0 | 0 0 | > c | > C | , 0 | . 0 | 0 | 0 | > |
| 훈 | green-brown | 000 | 0 | 00 | 00 | 0 | 0 0 | 0 | 0 0 | 0 | 0 | 00 | 0 | o c | 0 | 0 | 0 0 | > c | > C | , 0 | - | - | 0 | > |
| | plue-green | 12-70 | 4 | 00 | 00 | 0 | 0 0 | 0 | 0 0 | 0 | 0 | 0 0 | 0 | > C | 0 | 0 | 0 0 | > c | · c | , 0 | - | - | 0 | , |
| | Sphene |) - O - C | 0 | 00 | 00 | 0 | 0 0 | 0 | ۰, | 0 | 0 | 0 - | 8 | | - 0 | 0 | m (| N C | , c | , 0 | - | 0 | 0 | > |
| | Staurolite | 0 4 - 0 0 | 1 00 | ი – | ← 70 | 0 | - 0 | 0 | 0 0 | 0 | 0 | 00 | 0 | o c | 0 | 0 | ۰, | - c | > - | | 0 | 0 | 0 0 | y |
| | Rutile | 0046 | 1 - | - 4 | | - | 0 0 | · - | 0 0 | 0 | ო | 0 - | 0 | o c | - | 0 | | - c | ۰ د | 10 | - | 0 | 0 0 | 2 |
| | Tourmaline | 0 4 4 4 | 20 | 13 | 22 | 16 | 12 | 1 8 | 6 7 | 31 | 12 | 9 7 | 7 | | 4 | 2 | , | ۰ ، | , , | . ლ | 10 | 17 | ٠ س | |
| | Zircon | 4 0 4 4 | , v | 6 4 | 22 | ω : | ٥ د | ω . | ۵ ۵ | 2 | 56 | ٦ و | 7 | ρα | ^ | ო : | ٥, | ۰ ۵ | 1 0 | : 2 | 2 | 15 | 30 | 3 |
| | Apatite | 63 37 87 87 | 38 | 60 | 49 | 29 | 62 | 6 1 | 28 | 9 | 48 | 86 | 25 | 4 4 | 4 0 | 6 | 2 5 | 7 7 | - 6 | 67 | 29 | 57 | 65 | 3 |
| | Total | . C . v . 4 | - 6 | | 0 4 | 9 , | 9 % | 2 + | 65 | 4 | Ξ | 29 | 57 | 8 9 | 8 4 | 73 | 67 | - 6 | 2 4 | , ω | ∞ | 7 | 0 4 | 2 |
| | Composite grains | 0000 | - | 00 | 00 | 0 | 0 0 | 0 | ۰ - | 0 | 0 | 0 - | 0 | ט ע | 0 | - | ω . | - 0 | , - | . 0 | - | 0 | 0 | 2 |
| Epidote Group | Saussurite | 0000 | 0 | 00 | 00 | 0 | 0 0 | 0 | - c | 0 | 0 | 00 | 0 | o c | 0 | 0 | - (| > c | , c | , 0 | 0 | 0 | 0 0 | , |
| ote G | Allanite | 0000 | 0 | 00 | 00 | 0 | 0 0 | 0 | 0 0 | 0 | 0 | 00 | 0 | - | . 0 | 0 | 0 0 | > < | , 0 | 0 | 0 | 0 | 0 0 | , |
| Epid | SpisioS | -000 | 4 | 00 | 00 | 0 | 0 0 | 0 | N C | 0 | 0 | 0 0 | 0 | - c | 0 | 0 | 0 0 | > c | , c | . 0 | 0 | • | 0 0 | > |
| | Clinozoisite | | 0 0 | 00 | 0 - | - (| ه د | ٠- | о С | - | ი . | o – | 9 1 | ח ער | , m | - (| 30 U | 0 0 | 1 10 | 0 | 0 | _ | 0 - | - |
| | Epidote | 9 9 9 6 - | - 2 | | N 60 | 5. | 9 6 | 9 5 | 53 | ო | ω . | 27 | 51 | 7 4 | 4 3 | 7 | 200 | 2 2 | 2 6 | , ω | 7 | 9 | 0 1 | |
| | Sample Depth (m) | 2050 2100 2125 | 2171 | 2200 | 2275 | 2350 | 2400 | 2500 | 2550 | 2650 | 2700 | 2750 | 2850 | 2950 | 3000 | 3100 | 3150 | 3200 | 3300 | 3350 | 3400 | 3500 | 3550 | 2000 |

Table 3 (continued)

| | Anatase & Brookite | 0 0 | 0 | 0 | 0 | N - | 0 | 0 | 0 | - | - | 0 + | - | - 0 | - | 0 | - | - | 0 | 0 | ۰ ، | - (| 0 0 | N | 0 0 | > C | > + | - 0 | , 0 |
|----------------|----------------------|------|------|------|------|------|------|------|------|------|------|------|--------------|------|------|------|------|------|------|------|------|----------------|------|----------------|------|---------------|----------------|---------------|--------------|
| | Garnet | 98 | | | | | | | | | | | | | | | | | | | | 2 . | | B 9 | 12 | ۶ ۵ | <u> </u> | - 0 | 2 0 |
| | IstoT | 100 | 100 | 100 | 100 | 1 00 | 100 | 100 | 100 | 100 | 100 | 9 6 | 5 5 | 100 | 100 | 100 | 100 | 36 | 33 | 42 | 17 | 5 . | 40 | 77 | 67 | 2 6 | 3 a | 400 | 9 6 |
| | Others | 0 0 | 0 | 0 | 0 (| o - | 0 | 0 | 0 | 0 | 0 | 0 | o c | 0 | 0 | - | 0 | - | 0 | 0 | 0 0 | э· | - (| <u> </u> | 0 | > + | - c | <u> </u> | 0 0 |
| | Serpentine | 00 | 0 | 0 | 0 | 0 | 0 | 0 | 0 | 0 | 0 | 0 | o c | 0 | 0 | 0 | 0 | 0 | 0 | 0 | 0 0 | э ^с | 0 | o (| 0 | 5 C | > < | > < | , 0 |
| | Pumpellyite | 00 | 0 | 0 | 0 (| 0 0 | 0 | 0 | 0 | 0 | 0 | 0 0 | o c | 0 | 0 | 0 | 0 | 0 | 0 | 0 | 0 0 | э ⁽ | 0 | э ⁽ | 0 | - | > < | ه د | ه د |
| | Lawsonite | 00 | 0 | 0 | 0 (| 0 | 0 | 0 | 0 | 0 | 0 | 0 0 | o c | 0 | 0 | 0 | 0 | 0 | 0 | 0 | 0 (| 5 | 0 (| э [,] | 0 0 | > | > c | > c | 0 0 |
| | Blue sodic amphibole | 00 | 0 | 0 | 0 | 0 0 | 0 | 0 | 0 | 0 | 0 | 0 0 | o c | 0 | 0 | 0 | 0 | 0 | 0 | 0 | 0 0 | o (| 0 | э ⁽ | 0 0 | <u> </u> | > < | > c | o 0 |
| | Chromian spinel | 00 | 0 | 0 | 0 (| 0 | 0 | 0 | 0 | 0 | 0 | 0 | 5 C | 0 | 0 | 8 | 0 | 0 | - | 0 | ۰ , | - 1 | 0 (| o · | - 1 | 4 + | - • | - 0 | 9 O |
| g | Total | 0 0 | 0 | 0 | 0 (| 0 0 | 0 | 0 | 0 | 0 | 0 | 0 0 | o c | 0 | 0 | 0 | 0 | 0 | - | 0 | 0 (| э <u>;</u> | Ξ, | - ' | 0 0 | o (| > | 5 C | o 0 |
| e G | Diallage | 00 | 0 | 0 | 0 (| 0 0 | 0 | 0 | 0 | 0 | 0 | 0 | o c | 0 | 0 | 0 | 0 | 0 | 0 | 0 | 0 (| י כ | က | <u> </u> | 0 (| 0 (| > < | 5 C | o 0 |
| Pyroxene Group | Hypersthene | 0 0 | 0 | 0 | 0 (| 0 0 | 0 | 0 | 0 | 0 | 0 | 0 0 | o c | 0 | 0 | 0 | 0 | 0 | 0 | 0 | 0 | 5 | 0 | o , | 0 | 0 (| > | 5 | o 0 |
| <u>P</u> | Augite & Diopside | 00 | 0 | 0 | 0 | 0 0 | 0 | 0 | 0 | 0 | 0 | 0 | o c | 0 | 0 | 0 | 0 | 0 | - | 0 | 0 | э ⁽ | 9 | _ | 0 | 0 0 | - | 5 0 | o 0 |
| | Tremolite | 00 | 0 | 0 | 0 | 00 | 0 | 0 | 0 | 0 | 0 | 0 0 | o c | 0 | 0 | 0 | 0 | 0 | 0 | 0 | 0 | o , | 0 | o , | 0 (| 0 (| > | 5 6 | o 0 |
| | letot | 0 0 | 0 | 0 | 0 | 0 0 | 0 | 0 | 0 | 0 | 0 | 0 | - | 0 | - | 0 | 0 | - | ო | N | 0 | o | ი (| <u> </u> | - (| 0 0 | - | - | o c |
| nde | other types | 00 | 0 | 0 | 0 | 0 0 | 0 | 0 | 0 | 0 | 0 | 0 | o c | 0 | 0 | 0 | 0 | 0 | 0 | 0 | 0 | <u> </u> | 0 | 0 | 0 | 0 0 | - | - | o 0 |
| Hornblende | prown | 00 | 0 | 0 | 0 | 0 0 | 0 | 0 | 0 | 0 | 0 | 0 0 | 0 | 0 | 0 | 0 | 0 | 0 | 0 | 0 | 0 | o | - (| 0 | 0 | 0 (| - | 5 0 | o 0 |
| 운 | green-brown | 0 0 | 0 | 0 | 0 | 0 0 | 0 | 0 | 0 | 0 | 0 | 0 | o c | 0 | 0 | 0 | 0 | 0 | ო | N | 0 | o | CI (| 0 | - | 0 | - | - | o 0 |
| | plue-green | 00 | 0 | 0 | 0 | 0 0 | 0 | 0 | 0 | 0 | 0 | 0 0 | o c | 0 | - | 0 | 0 | - | 0 | 0 | 0 | 5 | 0 | 0 | 0 | 0 (| 5 (| 5 6 | o 0 |
| | Sphene | 0 0 | 0 | 0 | 7 | 0 - | ო | - | - | - | - | 0 | o c | 0 | 0 | 0 | 0 | _ | 0 | 0 | 0 | 5 | 0 | 0 | 0 | 0 (| > (| 5 0 | 5 0 |
| | Staurolite | ၀ ဖ | 0 | 0 | 9 | 0 0 | 0 | 0 | 0 | 0 | 0 | 0 0 | o c | 0 | 0 | - | 0 | 0 | 0 | 0 | 0 | - | 0 | 0 | 0 | 0 (| > c | 5 6 | 5 0 |
| | Rutile | - m | 0 | 0 | 0 | - 0 | - | 0 | - | - | 0 | 0 0 | o + | - 0 | 0 | 8 | 0 | 0 | - | - | 0 | _ | - 1 | 0 | 0 | 2 1 | Ω , | <u></u> | വ |
| | Tourmaline | 7 | 15 | 9 | φ : | - 9 | က | 7 | 14 | œ | 12 | 13 | ٥ , | 0 0 | 26 | 28 | 16 | ი | თ | 9 | - ' | 9 | ٧, | æ ; | 50 | 47 | 2, | - ; | 4 - 45 |
| | Zircon | 32 | 12 | 10 | 9 9 | 8 4 | 4 | 8 | | | | | | | | | | | | | | | | | | | | - | 4 7 4 7 |
| | Apatite | 53 | 68 | 7 | 20 | 23 | 13 | Ξ | 52 | 40 | 53 | 76 | د بر د بر | 73 | 29 | 54 | 64 | æ | 10 | 4 | ω : | <u> </u> | ω (| 80 | 56 | 2 . | » · | 4 (| ၁ က |
| | Total | ~ ღ | 2 | 13 | 26 | 0 2 | 99 | 84 | 25 | 46 | 28 | ro o | o a | ۰ ۵ | က | - | თ | ^ | N | - | 0 | _ ' | 9 | 27 | - 1 | 0 | - | <u> </u> | o 0 |
| | Composite grains | 0 0 | 0 | 0 | - (| ۰ - | 0 | 0 | 0 | က | 0 | 0 0 | o c | 0 | 0 | 0 | 0 | 0 | 0 | 0 | 0 | <u> </u> | 0 | 0 | 0 | 0 | 5 | 5 6 | o 0 |
| Epidote Group | Saussurite | 00 | 0 | 0 | 0 | 0 0 | 0 | 0 | 0 | - | 0 | 0 0 | o c | 0 | 0 | 0 | 0 | 0 | 0 | 0 | 0 | <u> </u> | 0 | 0 | 0 | 0 (| - | 5 (| 00 |
| ote | Allanite | 00 | 0 | 0 | 0 (| 00 | 0 | 0 | 0 | 0 | 0 | 0 0 | o c | 0 | 0 | 0 | 0 | 0 | 0 | 0 | 0 | 5 | 0 | o · | 0 | 0 (| - | 5 | 5 0 |
| Epid | SpirioS | 00 | 0 | 0 | 0 | 0 0 | 0 | - | 0 | 0 | 0 | 0 | o c | 0 | 0 | 0 | 0 | 0 | 0 | 0 | 0 | 5 | 0 (| 0 | 0 | 0 (| 5 (| 5 (| 5 0 |
| | Olinozoisite | - 0 | 0 | 0 | ç , | O 10 | 21 | 17 | 9 | Ξ | ς, | 0 0 | ى د | ۰ ٥ | 0 | 0 | - | 8 | 0 | 0 | 0 | 0 | 0 | 0 | 0 | 0 (| o (| 5 (| 00 |
| | etobid∃ | ဖ က | 2 | Ξ | 45 | 0 7 | 45 | 99 | 9 | 31 | 23 | ഗ | 5 (| o 0 | က | - | æ | လ | Q | - | 0 | - | 9 | 21 | - | 0 (| o (| 5 (| 5 0 |
| | Sample Depth (m) | 3650 | 3750 | 3800 | 3850 | 3900 | 4000 | 4050 | 4100 | 4150 | 4200 | 4250 | 4350 | 4450 | 4500 | 4550 | 4700 | 4750 | 4796 | 4840 | 4860 | 4934 | 4950 | 4974 | 5015 | 5050 | 5130 | 5155 | 5175 5176 |

Table 3 (continued)